J. Fluid Mech. (2003), *vol.* 476, *pp.* 115–157.
DOI: 10.1017/S0022112002002902 Printed in the United Kingdom

Drag, deformation and lateral migration of a buoyant drop moving near a wall

By JACQUES MAGNAUDET[1], SHU TAKAGI[2] AND DOMINIQUE LEGENDRE[1]

[1]Institut de Mecanique des Fluides de Toulouse, UMR CNRS/INPT/UPS 5502, 2, Allée Camille Soula, 31400 Toulouse, France

[2]Department of Mechanical Engineering, The University of Tokyo 7-3-1 Hongo, Bunkyo, Tokyo 113-8656, Japan

(Received 6 March 2002 and in revised form 25 August 2002)

The problem of a drop of arbitrary density and viscosity moving close to a vertical wall under the effect of buoyancy is analysed theoretically. The case where the suspending fluid is at rest far from the drop and that of a linear shear flow are both considered. Effects of inertia and deformation are assumed to be small but of comparable magnitude, so that both of them contribute to the lateral migration of the drop. Expressions for the drag, deformation and migration valid down to separation distances from the wall of a few drop radii are established and discussed. Inertial and deformation-induced corrections to the drag force and slip velocity of a buoyant drop moving in a linear shear flow near a horizontal wall are also derived.

1. Introduction

Theoretical studies of wall–particle interactions in low-Reynolds-number flows began when Faxén (1921, 1924) derived a mathematical transformation by which Stokes flow solutions around a spherical particle may be expressed in an integral form enabling the no-slip boundary condition on a plane wall to be easily taken into account. Early studies focused on wall-induced corrections to the drag force in various geometries (see Happel & Brenner 1973 for a review). In a seminal series of experiments, Segré & Silberberg (1962*a*, *b*) demonstrated that small neutrally buoyant particles moving in a circular Poiseuille flow experience a lateral migration that tends to accumulate them in an annulus with a well-defined radius. This discovery, combined with the proof that Stokes-type solutions around a sphere cannot produce any lift force (Bretherton 1962), provided a strong stimulation for studying small inertia effects affecting rigid particles moving in wall-bounded shear flows. In a classical paper, Saffman (1965) established the expression for the lift force experienced by a sphere moving along the streamlines of an unbounded linear shear flow, under conditions where inertia effects due to the shear dominate those due to the slip velocity between the undisturbed flow and the sphere (see Stone 2000 for further developments of Saffman's theory). Nevertheless, Saffman's theory could not explain the observations of Segré & Silberberg (1962*a*, *b*) or those displayed by further experiments of the same type. Hence it became obvious that wall effects had to be explicitly taken into account in the determination of the lateral force experienced by the particle.

Cox & Brenner (1968) derived a general formal method allowing the migration velocity of a rigid particle to be obtained in the case where the particle Reynolds

number is small compared to unity and the walls lie in the Stokes region of the flow disturbance produced by the particle. A crucial point recognized in their investigation is that, under the assumptions stated above, first-order inertial effects affecting particles moving in a certain class of flows may be obtained through a regular expansion with respect to the Reynolds number because wall-induced corrections make the velocity disturbance decay as r^{-2} in the far field of the particle instead of decaying as r^{-1} in the classical unbounded case (r denotes the distance from the centre of the particle). Under similar assumptions, Ho & Leal (1974) combined the use of Faxén's transformation with that of a suitable form of Lorentz's (1896) reciprocal theorem to evaluate the leading-order contribution to the migration velocity of a neutrally buoyant particle moving in a plane Couette or Poiseuille flow. This allowed them to predict that in Couette flow the equilibrium position of the particle lies on the centreline, whereas in Poiseuille flow there are two symmetric stable equilibrium positions located at approximately 0.6 times the channel half-width from the centreline. These predictions agree with the experimental observations of Halow & Wills (1970) and Segré & Silberberg (1962*a*, *b*), respectively. Vasseur & Cox (1976) and Cox & Hsu (1977) applied the general technique of Cox & Brenner (1968) to study the migration of a rigid particle in various flows bounded by a single wall or by two walls. Their results include the case where the fluid is at rest far from the particle, as well as plane Couette and Poiseuille flows. Surprisingly, while the results of Vasseur & Cox (1976) and Ho & Leal (1974) are in reasonable agreement in the core of Couette and Poiseuille flows, for reasons that are unclear they disagree significantly as the walls are approached.

The case where the wall lies in the Oseen region of the flow disturbance, i.e. viscous and inertia effects have a comparable magnitude near the wall, was studied by Vasseur & Cox (1977) and McLaughlin (1993) for the situation of a fluid at rest far from the particle and for a linear shear flow, respectively. Following Saffman (1965), they determined the far-field disturbance by employing a point-force approximation and used this outer solution to evaluate the force acting on the particle. This allowed them to obtain the migration velocity of the particle and the wall-induced drag correction as a function of the distance to the wall. A similar technique was used for Poiseuille flow by Schonberg & Hinch (1989) who showed that increasing the channel Reynolds number makes the equilibrium position of the particle move towards the wall, as observed by Segré & Silberberg (1962*a*, *b*). Over the last two decades many other theoretical investigations of the migration of buoyant or neutrally buoyant rigid particles moving in linear or quadratic wall-bounded shear flows have been carried out. The various contributions differ in the base flow they consider and in the assumptions under which the results are derived. A comprehensive discussion of these contributions and of their range of validity is provided by Hogg (1994).

Deformable drops and bubbles moving in shear flows or in wall-bounded flows may also experience a lateral migration, even in the zero-Reynolds-number limit (Leal 1980). At first glance, both the governing equations and the boundary conditions are linear in this case. However, the fact that the matching of velocities and stresses through the drop surface must be satisfied on a deformed interface whose shape is part of the solution of the problem induces a nonlinearity which may result in a lift force. Existence of such a lateral force in wall-bounded shear flows was clearly proved in several Couette flow experiments (e.g. Karnis, Goldsmith & Mason 1966; Karnis & Mason 1967; Chan & Leal 1981; Smart & Leighton 1991) as well as in numerical studies making use of the boundary integral technique (Uijttewaal, Nijhof & Heethaar 1993; Uijttewaal & Nijhof 1995). The problem was first worked out analytically by Chaffey, Brenner & Mason (1965) who predicted that a neutrally

buoyant drop moving in a linear shear flow bounded by a single wall migrates away from the wall with a migration velocity decreasing inversely with the square of the separation distance between the drop and the wall. This problem was revisited and broadened by Chan & Leal (1979) who considered the case of both Couette and Poiseuille flows and included possible non-Newtonian effects of the suspending fluid and corrections due to channel curvature. Chan & Leal combined the use of the technique of domain perturbations with that of a suitable form of the reciprocal theorem from which the migration velocity of the drop may be directly expressed in the form of surface integrals on the undeformed drop surface. Their result for a plane Couette flow of a Newtonian fluid essentially agrees with that of Chaffey *et al.* (1965). For a Poiseuille flow of a Newtonian fluid, their prediction shows that the migration velocity decreases inversely with the separation distance between the drop and the wall; it also indicates that the direction of the lateral migration depends on the viscosity ratio between the two fluids, and is directed towards the wall when the two viscosities are comparable. Chan & Leal (1981) subsequently confirmed several of their theoretical predictions, especially those related to curvature effects, by analysing new experimental data obtained in a rotating Couette viscometer.

The above review highlights the fact that in available theoretical studies, inertial effects have essentially been considered in the particular case of rigid particles. The only work known to us where inertial effects have been considered for drops and bubbles concerns the case of a spherical drop in a quadratic flow (Chan & Leal 1977), the generalization of Saffman's (1965) result to spherical drops and bubbles in an unbounded linear shear flow (Legendre & Magnaudet 1997), and the extension of the result of Vasseur & Cox (1977) to an inviscid spherical bubble moving in a quiescent liquid (Takemura *et al.* 2002). The reason for this lack is that most experiments carried out to date have used a very viscous suspending liquid (with a viscosity typically 10^3 times larger than that of water) and almost neutrally buoyant drops, because their primary aim was to improve the understanding of suspension rheology. For this reason the particle Reynolds number was often several orders of magnitude smaller than the capillary number, making deformation-induced migration dominant. Nevertheless, recent experiments carried out by Takemura *et al.* (2002) with bubbles rising in silicone oils of various viscosities have shown that the contribution of inertia to the migration of millimetric bubbles is larger than or of the same order as that of deformation for oils with a viscosity up to one hundred times that of water. This makes clear the fact that in liquids of moderate viscosity, a reliable prediction of the lateral migration of drops and bubbles generally requires effects of inertia to be taken into account consistently with those of deformation.

Another limitation of most of the available predictions of wall-induced drag and lift on particles and drops is that they are generally valid only at distances from the closest wall larger than typically ten particle radii because only the leading-order contribution of the wall effect is evaluated. This is due on the one hand to the tediousness of the calculations, and on the other hand to the fact that in most studies the focus has been on the prediction of the particle distribution in the core of the flow, especially on the determination of equilibrium positions, rather than on the particle motion close to the wall. Nevertheless there are many areas of two-phase flows where the knowledge of forces acting on drops and particles moving at low Reynolds number close to a wall, i.e. at separation distances only slightly larger than the particle radius, is of importance. These include deposition of droplets and particles on walls, bubbly flows in tubes, near-wall motion of drops in packed columns, motion of particles in boundary layers, nucleate boiling on superheated walls, etc.

Such situations are intermediate between those already treated in the contributions discussed above and those in which the gap between the particle and the wall is so small that the leading-order effect of the interaction must be evaluated by using specific approximations taking into account the lubrication layer in the gap (see O'Neill & Stewarson 1967 and Goldman, Cox & Brenner 1967 for the drag and rotation of a rigid particle in this regime, Leighton & Acrivos 1985 and Krishnan & Leighton 1995 for the inertial lift on a rigid sphere in contact with a wall). In contrast with the case of a distant wall where the particle may be treated as a point-force because its radius is negligible compared to the separation distance, dealing with such intermediate situations requires the finite size of the particle to be taken into account. In other words, in order for the solution to be valid fairly close to the wall it is necessary to consider higher-order contributions in the multipole expansion of the flow disturbance induced by the particle as well as in the interaction process with the wall. Assuming that the wall lies in the Stokes region of the flow disturbance, Cherukat & McLaughlin (1994) and Becker, McKinley & Stone (1996) followed such an approach to determine the inertial lift force on a rigid sphere translating near a wall in a linear shear flow and in a fluid at rest, respectively (actually the main focus of Becker *et al.* was on non-Newtonian near-wall effects but they also considered inertial corrections to the Newtonian situation). Starting from an exact solution of Stokes equation valid whatever the distance between the particle and the wall, both groups used the reciprocal theorem and evaluated numerically the corresponding volume integral to obtain the lift force as a function of the distance to the wall.

The aim of the present contribution follows from the previous two remarks. Our goal is to provide a consistent treatment of first-order inertial and deformation effects on a drop of arbitrary viscosity moving almost parallel to a wall bounding a Newtonian fluid, the 'film' thickness between the drop and the wall being typically of the same order of magnitude as the drop radius. We consider in detail the situation where the fluid is at rest far from the drop, the motion of which is driven by buoyancy. Results with a more limited domain of validity (in terms of separation distance) are also derived for the case of a uniform shear flow. The situation of a buoyant drop moving in a linear shear flow near a horizontal wall is also briefly examined. The solution procedure employed throughout the present investigation makes intensive use of three classical mathematical tools. The exact boundary conditions on the deformed drop surface are expanded into an infinite series of conditions on the undeformed drop by using the technique of domain perturbations (Leal 1992, pp. 223–229, and Manga & Stone 1993). To obtain the zero-Reynolds-number velocity disturbance induced by the drop in the presence of the wall, we employ the method of reflections and use Faxén's transformation to satisfy the no-slip condition at the wall (see Happel & Brenner 1973, chap. 7, and Ho & Leal 1974). Finally, the lateral force is found by writing an appropriate form of the reciprocal theorem and evaluating the corresponding surface and volume integrals in which only the zero-Reynolds-number solution about the undeformed drop in involved (Ho & Leal 1974; Chan & Leal 1979; Manga & Stone 1993).

The structure of the paper is as follows. In § 2 we formulate the problem and derive the governing equations at the required order of approximation. The zeroth-order solution for a drop in creeping motion parallel to the wall is obtained in § 3, along with expressions for the wall-induced drag force and deformation. In § 4 we solve the so-called complementary problem of a spherical drop in creeping motion perpendicular to the wall. The solution of this problem is required to obtain the lift (or migration) force acting on the drop through the use of the reciprocal theorem.

The form of this theorem suitable for obtaining the inertial and deformation-induced contributions to the lift force and the evaluation of the latter contribution are described in § 5. Section 6 is devoted to the evaluation of the inertial lift force and to a short discussion of the total force. Section 7 gives a brief account of the case of a buoyant drop moving near a horizontal wall. A summary of the main results of this investigation is given in § 8. Readers mainly interested in zero-Reynolds-number results (drag and deformation) may concentrate on § 3 (resp. § 4) for the case of a drop moving parallel (resp. perpendicular) to the wall. Those looking for characteristics of the lateral migration may focus on § 5 (resp. § 6) for deformation-induced (resp. inertial) migration near a vertical wall, and on § 7 for corresponding results near a horizontal wall. Moreover, most results obtained in this work for the two extreme cases of a bubble filled with a gas of negligible viscosity and a rigid sphere are summarized in table 2 in § 8; the corresponding equation in the text for a drop of arbitrary viscosity is also indicated in these tables.

2. Governing equations

We consider a drop of a Newtonian fluid of density $\tilde{\rho}$ and viscosity $\tilde{\mu}$ moving in a suspending Newtonian fluid of density ρ and viscosity μ under the effect of gravity g (the effect of a non-zero shear rate $\dot{\gamma}$ will be introduced later). The drop has an undeformed radius R and moves at a time-dependent distance L from an infinite vertical wall. Our goal is to find how the presence of the wall affects the shape and trajectory of the drop in situations where deformation and inertial effects are small, the density ratio $\bar{\rho} = \tilde{\rho}/\rho$ and the viscosity ratio $\lambda = \tilde{\mu}/\mu$ being arbitrary (see however the remark at the end of § 3.1). To write down the governing equations of the problem, we normalize distances by the undisturbed radius R and velocities by the viscous-gravitational scale $\rho|1-\bar{\rho}|R^2g/\mu$; this choice ensures that the vertical velocity of the drop is of order unity whatever the distance L to the wall. Then the first two relevant control parameters of the problem are the Bond number $\delta = \rho|1-\bar{\rho}|R^2g/\gamma$, γ denoting surface tension, and the Galileo number $G = \rho^2|1-\bar{\rho}|gR^3/\mu^2$. These parameters compare the buoyancy force to capillary and viscous effects, respectively. Note that they play the role of the more familiar capillary and Reynolds numbers in the present buoyancy-driven situation. We assume that δ, G and $(\bar{\rho}/\lambda)G$ are small compared to unity and that the first two are *a priori* of a similar order of magnitude, i.e. the Ohnesorge number $Oh = G/\delta = \rho R\gamma/\mu^2$ is $O(1)$. The presence of the wall introduces a third parameter into the problem, namely the length ratio $\kappa = R/L$ which compares the radius of the drop with the distance separating it from the wall. All the dimensionless parameters defined above, as well as some others to be introduced below, are listed in table 1.

In addition to the previous assumptions we also assume that time plays no direct role in the present problem. This is reasonable because the dimensionless migration velocity V_M is expected to be much smaller than unity, so that the corresponding time scale $\mu/(\rho|1-\bar{\rho}|RgV_M)$ is larger by factor V_M^{-1} than the viscous-gravitational time scale $\mu/(\rho|1-\bar{\rho}|Rg)$, which itself is larger by a factor G^{-1} than the viscous time scale $\rho R^2/\mu$ (the magnitude of transient effects will be re-examined in § 7 in the case of a buoyant drop moving near a horizontal wall). Therefore the only effect of the time variation of L is to produce a quasi-steady drag force in the direction normal to the wall. We use a Cartesian coordinate system $(Ox_1x_2x_3)$ centred at the centroid O of the drop and moving with it, with x_1 directed upwards and x_3 perpendicular to the wall and directed away from it; the unit vectors corresponding to directions

Name	Definition	Interpretation
Density ratio	$\bar{\rho} = \tilde{\rho}/\rho$	Governs the magnitude of buoyancy effects
Viscosity ratio	$\lambda = \bar{\mu}/\mu$	Governs the entrainment of the inner fluid
Inverse of separation	$\kappa = R/L$	Compares the particle size to the distance to the wall
Bond number	$\delta = \rho\|1-\bar{\rho}\|R^2 g/\gamma$	Compares buoyancy effects to capillary effects
Galileo number	$G = \rho^2\|1-\bar{\rho}\|gR^3/\mu^2$	Compares buoyancy effects to viscous effects
Ohnesorge number	$Oh = G/\delta$	Compares capillary effects to viscous effects
Dimensionless shear rate	$\alpha = \mu\dot{\gamma}/\rho\|1-\bar{\rho}\|Rg$	Compares the imposed shear rate to the buoyancy-induced shear
	$R_\mu = (2+3\lambda)/2(1+\lambda)$	Strength of the Stokeslet in the unbounded solution
	$D_\mu = \lambda/4(1+\lambda)$	Strength of the dipole in the unbounded solution
	$R_\mu = 1/2(1+\lambda)$	Mobility of the inner fluid in the unbounded solution
	$R_S = (2+5\lambda)/2(1+\lambda)$	Strength of the stresslet in presence of a linear shear

TABLE 1. Definition and interpretation of the dimensionless parameters of the problem.

x_1, x_2 and x_3 are $\boldsymbol{e}_1$, $\boldsymbol{e}_2$ and $\boldsymbol{e}_3$, respectively (figure 1). Note that with this choice of coordinates the wall is located at $x_3 = -1/\kappa$.

Using the previous assumptions and keeping in mind that the drop can deform only if the Bond number δ is non-zero, we assume that the shape of the interface may be expanded in the form

$$r = 1 + \delta f^{(\delta)}\left(\frac{x_1}{r}, \frac{x_2}{r}, \frac{x_3}{r}\right) + \delta^2 f^{(\delta\delta)}\left(\frac{x_1}{r}, \frac{x_2}{r}, \frac{x_3}{r}\right) + \delta G f^{(\delta G)}\left(\frac{x_1}{r}, \frac{x_2}{r}, \frac{x_3}{r}\right) + \cdots, \quad (1)$$

where $r = \|\boldsymbol{x}\| = (x_1^2 + x_2^2 + x_3^2)^{1/2}$ and $f^{(\delta)}$, $f^{(\delta\delta)}$, $f^{(\delta G)}\ldots$ are unknown functions which depend only on the angular position along the drop surface. With these notation and definitions, the governing equations of the problem in the case where the fluid is at rest at infinity are

$$\left.\begin{aligned}
&\nabla\cdot\boldsymbol{U} = 0, \quad \nabla\cdot\tilde{\boldsymbol{U}} = 0,\\
&\nabla\cdot\boldsymbol{\Sigma} = G\boldsymbol{U}\cdot\nabla\boldsymbol{U}, \quad \nabla\cdot\tilde{\boldsymbol{\Sigma}} = \frac{\bar{\rho}G}{\lambda}\tilde{\boldsymbol{U}}\cdot\nabla\tilde{\boldsymbol{U}},\\
&\boldsymbol{U} = -\boldsymbol{V}_B \quad \text{for} \quad x_3 = -1/\kappa,\\
&\boldsymbol{U} \to -\boldsymbol{V}_B \quad \text{for} \quad r \to \infty,\\
&\left.\begin{aligned}
&\boldsymbol{U}\cdot\boldsymbol{n} = \tilde{\boldsymbol{U}}\cdot\boldsymbol{n} = 0\\
&\boldsymbol{n}\times\boldsymbol{U} = \boldsymbol{n}\times\tilde{\boldsymbol{U}}\\
&\boldsymbol{\Sigma}\cdot\boldsymbol{n} = \lambda\tilde{\boldsymbol{\Sigma}}\cdot\boldsymbol{n} - \frac{1-\bar{\rho}}{|1-\bar{\rho}|}x_1\boldsymbol{n} + \frac{1}{\delta}(\nabla\cdot\boldsymbol{n})\boldsymbol{n}
\end{aligned}\right\} \quad \text{for} \quad r = 1 + \delta f^{(\delta)} + \cdots,
\end{aligned}\right\} \quad (2a)$$

where $\boldsymbol{\Sigma} = -P\boldsymbol{I} + \nabla\boldsymbol{U} + \nabla^T\boldsymbol{U}$ (resp. $\tilde{\boldsymbol{\Sigma}} = -\tilde{P}\boldsymbol{I} + \nabla\tilde{\boldsymbol{U}} + \nabla^T\tilde{\boldsymbol{U}}$) is the stress tensor in the outer (resp. inner) fluid (P and $\tilde{P}$ begin the corresponding modified pressures), $\boldsymbol{U}$ (resp. $\tilde{\boldsymbol{U}}$) is the velocity in the outer (resp. inner) fluid evaluated in the moving frame, $\boldsymbol{V}_B$ is the absolute velocity of the drop centroid, and $\boldsymbol{n}$ is the unit normal to the interface directed into the suspending fluid. The last of (2a) may be integrated over the drop surface to obtain an integral momentum balance. The momentum equation

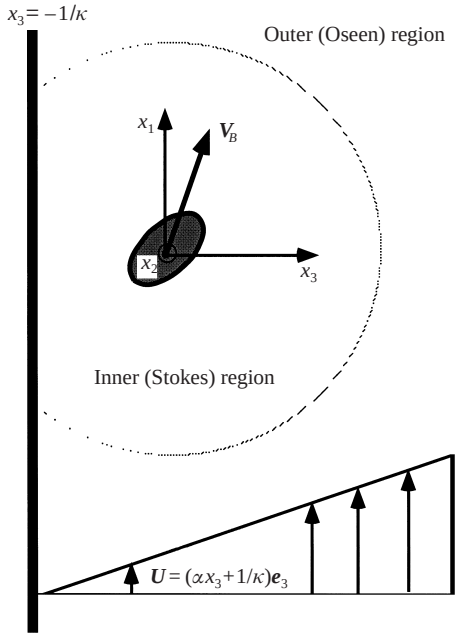

FIGURE 1. Sketch of the problem.

within the drop and the kinematic boundary condition at its surface imply that $\tilde{\boldsymbol{\Sigma}}$ does not contribute to this integral balance; the constraint of constant surface tension (no Marangoni effect) then yields the force balance

$$\int_{A_B} \boldsymbol{\Sigma} \cdot \boldsymbol{n} \, \mathrm{d}S = -\frac{4}{3}\pi \frac{1-\bar{\rho}}{|1-\bar{\rho}|} \boldsymbol{e}_1, \tag{2b}$$

where A_B denotes the drop surface.

We assume that variables $\Phi = (\boldsymbol{U}, \tilde{\boldsymbol{U}}, P, \tilde{P}, \boldsymbol{\Sigma}, \tilde{\boldsymbol{\Sigma}}, \boldsymbol{V}_B)$ can be expanded in the generic form $\Phi = \Phi^{(0)} + \delta\Phi^{(\delta)} + G\Phi^{(G)} + \delta^2\Phi^{(\delta\delta)} + \delta G\Phi^{(\delta G)} + G^2\Phi^{(GG)} + \cdots$. Actually, $\tilde{P}$ also contains an $O(1/\delta)$ term because the leading-order approximation to the pressure inside the drop must be $P_B = (1/\delta)\tilde{P}^{(1/\delta)} = 2/\delta$ in order to satisfy Laplace's law on the undeformed drop. Using (1), the kinematic and dynamic boundary conditions at the drop surface can be expanded in powers of δ and G (see Chan & Leal 1979 and Manga & Stone 1993 for details). This yields the leading-order problem of *creeping* flow around and inside a *spherical* drop:

$$\left.\begin{aligned}
&\nabla \cdot \boldsymbol{U}^{(0)} = 0, \quad \nabla \cdot \boldsymbol{\Sigma}^{(0)} = \boldsymbol{0}, \\
&\nabla \cdot \tilde{\boldsymbol{U}}^{(0)} = 0, \quad \nabla \cdot \tilde{\boldsymbol{\Sigma}}^{(0)} = \boldsymbol{0}, \\
&\boldsymbol{U}^{(0)} = -\boldsymbol{V}_B^{(0)} \quad \text{for} \quad x_3 = -1/\kappa, \\
&\boldsymbol{U}^{(0)} \to -\boldsymbol{V}_B^{(0)} \quad \text{for} \quad r \to \infty, \\
&\left.\begin{aligned}
&\boldsymbol{U}^{(0)} \cdot \boldsymbol{e}_r = \tilde{\boldsymbol{U}}^{(0)} \cdot \boldsymbol{e}_r = 0 \\
&\boldsymbol{e}_r \times \boldsymbol{U}^{(0)} = \boldsymbol{e}_r \times \tilde{\boldsymbol{U}}^{(0)} \\
&\boldsymbol{\Sigma}^{(0)} \cdot \boldsymbol{e}_r = \lambda \tilde{\boldsymbol{\Sigma}}^{(0)} \cdot \boldsymbol{e}_r - \frac{1-\bar{\rho}}{|1-\bar{\rho}|} x_1 \boldsymbol{e}_r - (2f^{(\delta)} + \nabla^2 f^{(\delta)})\boldsymbol{e}_r
\end{aligned}\right\} \quad \text{for} \quad r = 1,
\end{aligned}\right\} \tag{3a}$$

where $\boldsymbol{e}_r = \boldsymbol{x}/r$. The only non-zero component of $\boldsymbol{V}_B^{(0)}$ lies along the x_1-axis and is determined by the zeroth-order expansion of (2b), namely

$$\boldsymbol{F}_D = \int_{A_{B0}} \boldsymbol{\Sigma}^{(0)} \cdot \boldsymbol{e}_r \, \mathrm{d}S = -\tfrac{4}{3}\pi \frac{1-\bar{\rho}}{|1-\bar{\rho}|} \boldsymbol{e}_1, \tag{3b}$$

where $\boldsymbol{F}_D$ is the drag force on the drop and A_{B0} denotes the undeformed drop surface. Similarly, the governing equations of the $O(G)$ and $O(\delta)$ problems are found to be

$$\left.\begin{aligned}
&\nabla \cdot \boldsymbol{U}^{(G)} = 0, \quad \nabla \cdot \boldsymbol{\Sigma}^{(G)} = G\boldsymbol{U}^{(0)} \cdot \nabla \boldsymbol{U}^{(0)}, \\
&\nabla \cdot \tilde{\boldsymbol{U}}^{(G)} = 0, \quad \nabla \cdot \tilde{\boldsymbol{\Sigma}}^{(G)} = \frac{\bar{\rho} G}{\lambda} \tilde{\boldsymbol{U}}^{(0)} \cdot \nabla \tilde{\boldsymbol{U}}^{(0)}, \\
&\boldsymbol{U}^{(G)} = -\boldsymbol{V}_B^{(G)} \quad \text{for} \quad x_3 = -1/\kappa, \\
&\boldsymbol{U}^{(G)} \to -\boldsymbol{V}_B^{(G)} \quad \text{for} \quad r \to \infty, \\
&\left.\begin{aligned}
&\boldsymbol{U}^{(G)} \cdot \boldsymbol{e}_r = \tilde{\boldsymbol{U}}^{(G)} \cdot \boldsymbol{e}_r = 0 \\
&\boldsymbol{e}_r \times \boldsymbol{U}^{(G)} = \boldsymbol{e}_r \times \tilde{\boldsymbol{U}}^{(G)} \\
&\boldsymbol{\Sigma}^{(G)} \cdot \boldsymbol{e}_r = \lambda \tilde{\boldsymbol{\Sigma}}^{(G)} \cdot \boldsymbol{e}_r - (2f^{(\delta G)} + \nabla^2 f^{(\delta G)}) \boldsymbol{e}_r
\end{aligned}\right\} \quad \text{for} \quad r = 1;
\end{aligned}\right\} \tag{4a}$$

$$\left.\begin{aligned}
&\nabla \cdot \boldsymbol{U}^{(\delta)} = 0, \quad \nabla \cdot \boldsymbol{\Sigma}^{(\delta)} = \boldsymbol{0}, \\
&\nabla \cdot \tilde{\boldsymbol{U}}^{(\delta)} = 0, \quad \nabla \cdot \tilde{\boldsymbol{\Sigma}}^{(\delta)} = \boldsymbol{0}, \\
&\boldsymbol{U}^{(\delta)} = -\boldsymbol{V}_B^{(\delta)} \quad \text{for} \quad x_3 = -1/\kappa, \\
&\boldsymbol{U}^{(\delta)} \to -\boldsymbol{V}_B^{(0)} \quad \text{for} \quad r \to \infty, \\
&\left.\begin{aligned}
&\boldsymbol{U}^{(\delta)} \cdot \boldsymbol{e}_r - \boldsymbol{U}^{(0)} \cdot \nabla f^{(\delta)} + f^{(\delta)} \frac{\partial \boldsymbol{U}^{(0)}}{\partial r} \cdot \boldsymbol{e}_r \\
&\qquad = \tilde{\boldsymbol{U}}^{(\delta)} \cdot \boldsymbol{e}_r - \tilde{\boldsymbol{U}}^{(0)} \cdot \nabla f^{(\delta)} + f^{(\delta)} \frac{\partial \tilde{\boldsymbol{U}}^{(0)}}{\partial r} \cdot \boldsymbol{e}_r = 0 \\
&\boldsymbol{e}_r \times \left[\boldsymbol{U}^{(\delta)} + f^{(\delta)} \frac{\partial \boldsymbol{U}^{(0)}}{\partial r} \right] = \boldsymbol{e}_r \times \left[\tilde{\boldsymbol{U}}^{(\delta)} + f^{(\delta)} \frac{\partial \tilde{\boldsymbol{U}}^{(0)}}{\partial r} \right] \\
&\boldsymbol{\Sigma}^{(\delta)} \cdot \boldsymbol{e}_r - \boldsymbol{\Sigma}^{(0)} \cdot \nabla f^{(\delta)} + f^{(\delta)} \frac{\partial \boldsymbol{\Sigma}^{(0)}}{\partial r} \cdot \boldsymbol{e}_r \\
&\qquad = \lambda \left[\tilde{\boldsymbol{\Sigma}}^{(\delta)} \cdot \boldsymbol{e}_r - \tilde{\boldsymbol{\Sigma}}^{(0)} \cdot \nabla f^{(\delta)} + f^{(\delta)} \frac{\partial \tilde{\boldsymbol{\Sigma}}^{(0)}}{\partial r} \cdot \boldsymbol{e}_r \right] \\
&\qquad\quad + (2f^{(\delta)} + \nabla^2 f^{(\delta)}) \nabla f^{(\delta)} - (2f^{(\delta\delta)} + \nabla^2 f^{(\delta\delta)} \\
&\qquad\quad - 2(f^{(\delta)})^2 + \nabla f^{(\delta)} \cdot \nabla f^{(\delta)}) \boldsymbol{e}_r
\end{aligned}\right\} \quad \text{for} \quad r = 1.
\end{aligned}\right\} \tag{4b}$$

In addition, the $O(G)$ and $O(\delta)$ stress fields must satisfy the global constraint resulting from (2b), i.e.

$$\int_{A_{B0}} \boldsymbol{\Sigma}^{(G)} \cdot \boldsymbol{e}_r \, \mathrm{d}S = \int_{A_{B0}} \boldsymbol{\Sigma}^{(\delta)} \cdot \boldsymbol{e}_r \, \mathrm{d}S = \boldsymbol{0}. \tag{4c}$$

The goal is now to evaluate $\boldsymbol{V}_B^{(0)}$, $\boldsymbol{V}_B^{(\delta)}$ and $\boldsymbol{V}_B^{(G)}$ so that the force balances (2b) and (4c) are satisfied.

3. The drag and shape of the drop

3.1. *Solution at* $O(\kappa^3)$

To solve (3) we use the method of reflections (Happel & Brenner 1973, Chap. 7) and seek a solution of the form $\boldsymbol{U}^{(0)} = {}_1\boldsymbol{U}^{(0)} + {}_2\boldsymbol{U}^{(0)} + {}_3\boldsymbol{U}^{(0)} + \cdots$ where terms with an odd index are required to satisfy the boundary conditions at the drop surface, whereas terms with an even index result from the no-slip condition on the wall. This method assumes inherently that the separation between the drop and the wall is large, i.e. that κ is small compared to unity, so that the solution can be expanded in powers of κ. However, we shall see that solutions accurate up to $\kappa \approx 0.5$ may be obtained by stopping the expansion at $O(\kappa^3)$. The first term of the expansion is obviously the Hadamard–Rybczynski solution (Clift, Grace & Weber 1978, p. 33) for the unbounded flow around and inside a spherical drop, namely

$$ {}_1\boldsymbol{U}^{(0)} = V_{B1}^{(0)}\left[-\boldsymbol{e}_1 + \frac{R_\mu}{2}\left(\frac{\boldsymbol{e}_1}{r} + \frac{x_1\boldsymbol{x}}{r^3}\right) + D_\mu\left(\frac{\boldsymbol{e}_1}{r^3} - 3\frac{x_1\boldsymbol{x}}{r^5}\right)\right], \tag{5a} $$

$$ {}_1\tilde{\boldsymbol{U}}^{(0)} = M_\mu V_{B1}^{(0)}[(1-2r^2)\boldsymbol{e}_1 + x_1\boldsymbol{x}], \tag{5b} $$

where $V_{B1}^{(0)} = \boldsymbol{V}_B^{(0)} \cdot \boldsymbol{e}_1$ is the rise/fall velocity of the drop and

$$ R_\mu = \frac{2+3\lambda}{2(1+\lambda)}, \quad D_\mu = \frac{\lambda}{4(1+\lambda)} = \frac{R_\mu - 1}{2}, \quad M_\mu = \frac{1}{2(1+\lambda)} = \frac{R_\mu - 6D_\mu}{2}. \tag{6a} $$

Prefactors R_μ and D_μ determine the strength of the contributions of the stokeslet and irrotational dipole (or Stokes degenerate quadrupole), respectively, in the unbounded solution. In particular an inviscid bubble (i.e. a bubble filled with a gas of negligible viscosity, thus implying a zero-shear-stress interfacial condition in the suspending liquid) corresponds to $R_\mu = 1$, $D_\mu = 0$, while a rigid sphere is characterized by $R_\mu = 3/2$, $D_\mu = 1/4$. The factor M_μ characterizes the mobility of the fluid inside the drop and ranges from $1/2$ for an inviscid bubble to zero for a very viscous drop. These ratios play an important role in the present investigation, especially because they determine the strength of the various contributions involved in the expression for the drag and lift forces acting on the drop. Another prefactor to be frequently used below is

$$ R_S = R_\mu + 4D_\mu = \frac{2+5\lambda}{2(1+\lambda)}. \tag{6b} $$

Inserting the drag resulting from the velocity field (5*a*) into the force balance (3*b*) yields the Hadamard–Rybczynski formula $|V_{B1}^{(0)}| = (3R_\mu)^{-1}$. In the presence of the wall, the local value of $V_{B1}^{(0)}$ for finite κ differs from the above one, owing to wall interaction; the unbounded prediction is then valid only in the limit of large separations, i.e. $\kappa \to 0$. Hence it must be kept in mind that in the present problem $V_{B1}^{(0)}$ depends on κ.

To determine how the velocity field ${}_1\boldsymbol{U}^{(0)}$ is affected by the wall, it is particularly convenient to use Faxén's technique (Faxén 1921, 1924, see also Happel & Brenner 1973, p. 323, and Ho & Leal 1974). An outline of this technique is given in Appendix A and the images of the elementary solutions involved in the velocity fields ${}_2\boldsymbol{U}^{(0)}$ and ${}_4\boldsymbol{U}^{(0)}$ are determined there. Using (A 3)–(A 4) truncated at $O(\kappa^3)$, we find that the first reflection of the unbounded solution (5*a*) on the wall may be expressed near the drop

in the form

$$ {}_2\boldsymbol{U}^{(0)}(\kappa r \ll 1) = V_{B1}^{(0)}\{(I_D + D_\mu I_0)\boldsymbol{e}_1 + I_S(x_3\boldsymbol{e}_1 + x_1\boldsymbol{e}_3) + (\tfrac{1}{2}(I_{C2}+I_{C3})x_1^2 + I_{Q2}x_2^2 + I_{Q3}x_3^2)\boldsymbol{e}_1 - I_{C2}x_1x_2\boldsymbol{e}_2 - I_{C3}x_1x_3\boldsymbol{e}_3\} + O(\kappa^4), \tag{7} $$

where $I_D = R_\mu I'_D$, $I_S = R_\mu I'_S$, $I_{Q2} = R_\mu I'_{Q2}$, etc., the primed quantities and the prefactor I_0 being given by (A 3*b*) and (A 4*b*), respectively. After long but straightforward calculations, we obtain the velocity fields ${}_3\boldsymbol{U}^{(0)}$ and ${}_3\tilde{\boldsymbol{U}}^{(0)}$ required to satisfy the kinematic and dynamic boundary conditions at the drop surface, namely

$$ {}_3\boldsymbol{U}^{(0)} = -V_{B1}^{(0)}\left\{(I_D + D_\mu I_0)\left[\frac{R_\mu}{2}\left(\frac{\boldsymbol{e}_1}{r} + \frac{x_1\boldsymbol{x}}{r^3}\right) + D_\mu\left(\frac{\boldsymbol{e}_1}{r^3} - 3\frac{x_1\boldsymbol{x}}{r^5}\right)\right]\right. $$

$$ \left. + 2I_S\left[R_S\frac{x_1x_3\boldsymbol{x}}{r^5} + 2D_\mu\left(\frac{x_3\boldsymbol{e}_1}{r^5} + \frac{x_1\boldsymbol{e}_3}{r^5} - 5\frac{x_1x_3\boldsymbol{x}}{r^7}\right)\right] - \boldsymbol{V}_3\right\} + O(\kappa^4), \tag{8a} $$

$$ {}_3\tilde{\boldsymbol{U}}^{(0)} = M_\mu V_{B1}^{(0)}\{-(I_D + D_\mu I_0)[(1-2r^2)\boldsymbol{e}_1 + x_1\boldsymbol{x}] $$

$$ + I_S[(5r^2-3)(x_3\boldsymbol{e}_1 + x_1\boldsymbol{e}_3) - 4x_1x_3\boldsymbol{x}] + \tilde{\boldsymbol{V}}_3\} + O(\kappa^4), \tag{8b} $$

where R_S is defined by (6*b*), and $\boldsymbol{V}_3$ and $\tilde{\boldsymbol{V}}_3$ denote the $O(\kappa^3)$ terms associated with the quadratic contribution in ${}_2\boldsymbol{U}^{(0)}$. In the general case $\lambda \neq 0$, $\boldsymbol{V}_3$ (resp. $\tilde{\boldsymbol{V}}_3$) is composed of fifteen (resp. nine) terms, including a stokeslet of strength $-R_\mu D_\mu K_D$, with $K_D = I'_{C2} + I'_{C3} + 2(I'_{Q2} + I'_{Q3}) = \frac{1}{4}\kappa^3$. To save space, we do not write these terms explicitly. However, in the case of an inviscid bubble ($\lambda = 0$), the number of terms in $\boldsymbol{V}_3$ drops drastically and we have

$$ \boldsymbol{V}_3(\lambda = 0) = \frac{I_{Q2}}{4}\left(\frac{x_2^2\boldsymbol{e}_1}{r^5} - \frac{\boldsymbol{e}_1}{3r^3} + \frac{x_1\boldsymbol{x}}{r^5} - 5\frac{x_1x_2^2\boldsymbol{x}}{r^7}\right) $$

$$ + \frac{I_{Q3}}{4}\left(\frac{x_3^2\boldsymbol{e}_1}{r^5} - \frac{\boldsymbol{e}_1}{3r^3} + \frac{x_1\boldsymbol{x}}{r^5} - 5\frac{x_1x_3^2\boldsymbol{x}}{r^7}\right) - \frac{I_{C2}}{4}\left(\frac{x_1x_2\boldsymbol{e}_2}{r^5} + \frac{x_1\boldsymbol{x}}{r^5} - 5\frac{x_1x_2^2\boldsymbol{x}}{r^7}\right) $$

$$ - \frac{I_{C3}}{4}\left(\frac{x_1x_3\boldsymbol{e}_1}{r^5} + \frac{x_1\boldsymbol{x}}{r^5} - 5\frac{x_1x_3^2\boldsymbol{x}}{r^7}\right) $$

$$ + \frac{I_{C2}+I_{C3}}{8}\left(\frac{x_1^2\boldsymbol{e}_1}{r^5} - \frac{\boldsymbol{e}_1}{3r^3} + 3\frac{x_1\boldsymbol{x}}{r^5} - 5\frac{x_1^3\boldsymbol{x}}{r^7}\right) + \frac{K_D}{24}\left(\frac{\boldsymbol{e}_1}{r^3} - 3\frac{x_1\boldsymbol{x}}{r^5}\right). \tag{9} $$

From (8*a*) and (9) we see that the reflection of the stresslet on the wall produces terms of $O(\kappa^4)$, while that of the irrotational and Stokes quadrupoles contributes only at $O(\kappa^6)$. Consequently, only two additional reflections of the stokeslet are required to obtain the complete velocity field truncated at $O(\kappa^3)$. This remark and (7)–(8) allow us to conclude that the velocity field to be added to (5), (7)–(8) to obtain this approximation is

$$ \sum_{k=4}^{k=7} {}_k\boldsymbol{U}^{(0)} = V_{B1}^{(0)}\left\{I_D^2(1-I_D)\left[-\boldsymbol{e}_1 + \frac{R_\mu}{2}\left(\frac{\boldsymbol{e}_1}{r} + \frac{x_1\boldsymbol{x}}{r^3}\right) + D_\mu\left(\frac{\boldsymbol{e}_1}{r^3} - 3\frac{x_1\boldsymbol{x}}{r^5}\right)\right] - I_D I_S\right. $$

$$ \left. \times\left[(x_3\boldsymbol{e}_1 + x_1\boldsymbol{e}_3) - 2R_S\frac{x_1x_3\boldsymbol{x}}{r^5} - 4D_\mu\left(\frac{x_3\boldsymbol{e}_1}{r^5} + \frac{x_1\boldsymbol{e}_3}{r^5} - 5\frac{x_1x_3\boldsymbol{x}}{r^7}\right)\right]\right\} + O(\kappa^4), \tag{10a} $$

$$\sum_{k=5,7} {}_k\tilde{\boldsymbol{U}}^{(0)} = M_\mu V_{B1}^{(0)}\{I_D^2(1-I_D)[(1-2r^2)\boldsymbol{e}_1 + x_1\boldsymbol{x}]$$

$$-I_S I_D[(5r^2-3)(x_3\boldsymbol{e}_1 + x_1\boldsymbol{e}_3) - 4x_1x_3\boldsymbol{x}]\} + O(\kappa^4). \tag{10b}$$

The drag force may now be obtained by summing the strength of the stokeslets in (5*a*), (8*a*), (10*a*) and multiplying by $-4\pi V_{B1}^{(0)}$, or equivalently by applying Faxén's formula. In the present notation, Faxén's formula giving the drag force experienced by a drop moving in an arbitrary flow is (Hetsroni & Haber 1970; Kim & Karrila 1991, p. 78)

$$\boldsymbol{F}_D = 4\pi\{R_\mu(-\boldsymbol{V}_B^{(0)} + {}_2\boldsymbol{U}^{(0)}|_{\boldsymbol{x}=0} + {}_4\boldsymbol{U}^{(0)}|_{\boldsymbol{x}=0} + \cdots) + D_\mu\nabla^2({}_2\boldsymbol{U}^{(0)}|_{\boldsymbol{x}=0} + \cdots)\}. \tag{11}$$

Here this yields

$$\boldsymbol{F}_D = -4\pi V_{B1}^{(0)}\left\{R_\mu\left(\sum_{n=1}^{3}(-1)^n I_D^n - D_\mu(I_0 + K_D)\right)\right\}\boldsymbol{e}_1$$

$$= -4\pi R_\mu V_{B1}^{(0)}\left(1 + \tfrac{3}{8}R_\mu\kappa + \tfrac{9}{64}R_\mu^2\kappa^2 + \left(\tfrac{27}{512}R_\mu^3 - \frac{D_\mu}{2}\right)\kappa^3\right)\boldsymbol{e}_1 + O(\kappa^4). \tag{12}$$

All coefficients on the right-hand side of (12) are positive, implying that the drag is increased by the presence of the wall. This increase arises because as the drop moves along the wall, it displaces fluid and this displacement generates higher local strain rates compared to the unbounded situation, owing to the no-slip condition on the wall. The above expression for $\boldsymbol{F}_D$ may then be inserted into (3*b*) to obtain the rise/fall velocity $V_{B1}^{(0)}$ of the drop as a function of the dimensionless distance κ. We note that Shapira & Haber (1988) determined the $O(\kappa)$-correction to the drag for a drop moving in a quiescent liquid bounded by two parallel walls. When the drop is close to one of the walls, it can be shown that their correction tends to the factor $\frac{3}{8}R_\mu\kappa$ found in (12).

In the limit $\lambda \to 0$, (12) yields for an inviscid bubble

$$\boldsymbol{F}_D = -4\pi V_{B1}^{(0)}\left(1 + \tfrac{3}{8}\kappa + \tfrac{9}{64}\kappa^2 + \tfrac{27}{512}\kappa^3\right)\boldsymbol{e}_1 + O(\kappa^4). \tag{13a}$$

Similarly, Faxén's result for a solid sphere moving parallel to a wall (Happel & Brenner 1973, p. 327), is recovered by considering the limit $\lambda \to \infty$, in which case we obtain

$$\boldsymbol{F}_D = -6\pi V_{B1}^{(0)}\left(1 + \tfrac{9}{16}\kappa + \tfrac{81}{256}\kappa^2 + \tfrac{217}{4096}\kappa^3\right)\boldsymbol{e}_1 + O(\kappa^4). \tag{13b}$$

3.2. *The deformation at* $O(\kappa^3)$

Having determined the velocity field at $O(\kappa^3)$ we can now obtain the deformation $f^{(\delta)}$ at the same order of approximation. This requires evaluating the normal stress corresponding to the solution derived above and using the last of (3*a*). Since the normal stress produced by the unbounded solution (5*a*) and (5*b*) is exactly balanced by that due to the hydrostatic pressure (Batchelor 1967, p. 228), the deformation is only due to the normal stress produced by the linear and quadratic terms in ${}_{2k}\boldsymbol{U}^{(0)}(k \geqslant 1)$ and the associated terms in ${}_{2k+1}\boldsymbol{U}^{(0)}$ and ${}_{2k+1}\tilde{\boldsymbol{U}}^{(0)}$. Then, requiring that the centroid of the drop always coincides with the origin O of the coordinate system,

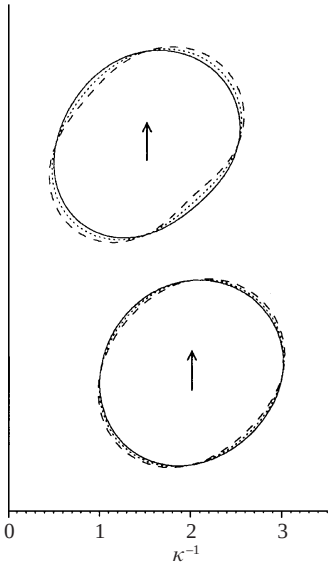

FIGURE 2. The shape of a deformed drop moving parallel to the wall as predicted by (14*b*) for $\kappa = 0.5$ and 0.67 (the rise/fall velocity is taken as unity and the Bond number is arbitrarily set to 0.5): ——, $\lambda = 0$; · · · · · ·, $\lambda = 1$; – – –, $\lambda \to \infty$.

we find

$$f^{(\delta)} = {}_2f^{(\delta)} + {}_3f^{(\delta)} + O(\kappa^4) = V_{B1}^{(0)}\Bigg\{(4R_\mu - 5D_\mu)I_S(1 - I_D)\frac{x_1x_3}{r^2} + \left(\tfrac{5}{4}R_\mu - 2D_\mu\right)\frac{x_1}{r}\left[\frac{I_{C2} + I_{C3}}{2}\left(\frac{x_1^2}{r^2} - \frac{3}{5}\right) + (I_{Q2} - I_{C2})\left(\frac{x_2^2}{r^2} - \frac{1}{5}\right) + (I_{Q3} - I_{C3})\left(\frac{x_3^2}{r^2} - \frac{1}{5}\right)\right]\Bigg\} + O(\kappa^4). \tag{14a}$$

Replacing the prefactors by their value and introducing the angular coordinates (θ, φ) such that $x_1/r = \cos\theta$, $x_2/r = \sin\theta\cos\varphi$, $x_3/r = \sin\theta\sin\varphi$, this result may also be expressed in the form

$$f^{(\delta)} = V_{B1}^{(0)}R_\mu\left\{\frac{3}{128}\frac{16 + 19\lambda}{1 + \lambda}\kappa^2\left(1 + \tfrac{3}{8}R_\mu\kappa\right)\sin 2\theta\sin\varphi + \frac{27}{10240}\frac{10 + 11\lambda}{1 + \lambda}\kappa^3[(5\cos 3\theta - \cos\theta)\sin^2\varphi + 4\cos\theta\cos^2\varphi]\right\} + O(\kappa^4). \tag{14b}$$

This deformation is due to the $O(\kappa^2)$ strain rate produced by the relative motion of the drop with respect to the wall. Predictions of (14*b*) are plotted in figure 2 for two different separation distances from the wall. Equation (14*b*) and figure 2 show that at the present level of approximation, the deformation of the drop is composed of two different modes. The first is due to the uniform strain associated with the first two reflections of the stokeslet on the wall. The corresponding deformation is maximum along the diagonals $x_3 = \pm x_1$ and takes the same form as that experienced by a drop held fixed in an unbounded linear shear flow (Taylor 1932, 1934). We shall refer to this mode as mode 2 since it produces two maxima in the local radius of the drop. The second mode, mode 3 say, results from the quadratic flow induced by the first reflection of the stokeslet on the wall; the deformation due to this mode

is symmetric with respect to the plane $x_3 = 0$. The prefactors $(16 + 19\lambda)/(1 + \lambda)$ and $(10 + 11\lambda)/(1 + \lambda)$ corresponding to each of these two modes are those found in previous studies dealing with drop deformation in linear and quadratic shear flows, respectively (e.g. equation (4.16*a*) of Chan & Leal 1979). We have compared the leading-order term in the right-hand side of (14*b*) with the result of Shapira & Haber (1988) who determined the mode-2 deformation of a drop moving between two parallel walls. It turns out that the present prediction agrees with their result in the limit case where the drop is close to one of the walls.

It must be kept in mind that, starting from an undeformed shape, the characteristic time required to reach the quasi-steady state described by (14*a*, *b*) increases linearly with $1 + \lambda$ for a given density ratio $\bar{\rho}$. Hence the present quasi-steady solution is reached in a much shorter time for an inviscid bubble than for a very viscous drop. Moreover the present solution is strictly valid only for $\lambda < O(1/\delta)$, since in the opposite limit $\lambda > O(1/\delta)$ the deformation is determined by the kinematic condition at the interface, rather than by the normal stress balance (Taylor 1934; Cox 1969; Frankel & Acrivos 1970). Hence in practice the solutions derived in this paper for the deformation and deformation-induced migration are essentially valid for $\lambda = O(1)$; when these solutions are discussed 'in the limit of a very viscous drop' it must be understood that we assume that conditions $\lambda \to \infty$, $\delta \to 0$, and $\lambda\delta \ll 1$ are satisfied.

3.3. *A higher-order approximation of drag and deformation*

The result (14*b*) is certainly accurate when the drop moves at some radii from the wall. In contrast, for small separations (κ larger than 1/3, say), higher-order contributions may change significantly the strength of the deformation. To improve the accuracy of the above results in this situation, while keeping the additional effort reasonable, we perform a partial expansion of the velocity field $\boldsymbol{U}^{(0)}$ up to terms of $O(\kappa^5)$. We select this order of approximation for two reasons. First it is clear that the reflection of the stresslet must be included in the process in order to improve the accuracy close to the wall. Since this reflection produces a stokeslet at $O(\kappa^4)$ and a new stresslet at $O(\kappa^5)$, improving the prediction of the deformation requires terms of $O(\kappa^5)$ to be considered. Second, the lowest-order term produced by the reflection of the irrotational and Stokes quadrupoles in (12*a*)–(13) is of $O(\kappa^6)$. To keep the calculations simple, we avoid considering this reflection by stopping the process at $O(\kappa^5)$.

Using results (A 5*a*, *b*) for the image of the stresslet involved in (8*a*) and considering five (resp. one) reflection(s) of the Stokeslet (resp. the dipole) of (5*a*) together with the various singularities induced by ${}_2\boldsymbol{U}^{(0)} + {}_4\boldsymbol{U}^{(0)} + \cdots$ and their own reflections, we can write the velocity field up to terms of $O(\kappa^5)$ in the condensed form

$$\sum_{k=1}^{k=11} {}_k\boldsymbol{U}^{(0)} = V_{B1}^{(0)}\Bigg\{K_{SD}\left[-\boldsymbol{e}_1 + \frac{R_\mu}{2}\left(\frac{\boldsymbol{e}_1}{r} + \frac{x_1\boldsymbol{x}}{r^3}\right) + D_\mu\left(\frac{\boldsymbol{e}_1}{r^3} - 3\frac{x_1\boldsymbol{x}}{r^5}\right)\right]$$
$$+K_{SS}\left[(x_3\boldsymbol{e}_1 + x_1\boldsymbol{e}_3) - 2R_S\frac{x_1x_3\boldsymbol{x}}{r^5} - 4D_\mu\left(\frac{x_3\boldsymbol{e}_1}{r^5} + \frac{x_1\boldsymbol{e}_3}{r^5} - 5\frac{x_1x_3\boldsymbol{x}}{r^7}\right)\right]$$
$$+K_R(x_3\boldsymbol{e}_1 - x_1\boldsymbol{e}_3) + \boldsymbol{U}_Q + \boldsymbol{T}_3 + \boldsymbol{T}_4 + \boldsymbol{T}_5\Bigg\} + O(\kappa^6), \tag{15a}$$

and

$$\sum_{k=1}^{k=5} {}_{2k+1}\tilde{\boldsymbol{U}}^{(0)} = V_{B1}^{(0)}\{M_\mu K_{SD}[(1 - 2r^2)\boldsymbol{e}_1 + x_1\boldsymbol{x}] + K_R(x_3\boldsymbol{e}_1 - x_1\boldsymbol{e}_3)$$
$$+M_\mu K_{SS}[(5r^2 - 3)(x_3\boldsymbol{e}_1 + x_1\boldsymbol{e}_3) - 4x_1x_3\boldsymbol{x}] + \tilde{\boldsymbol{T}}_3 + \tilde{\boldsymbol{T}}_4 + \tilde{\boldsymbol{T}}_5\} + O(\kappa^6), \tag{15b}$$

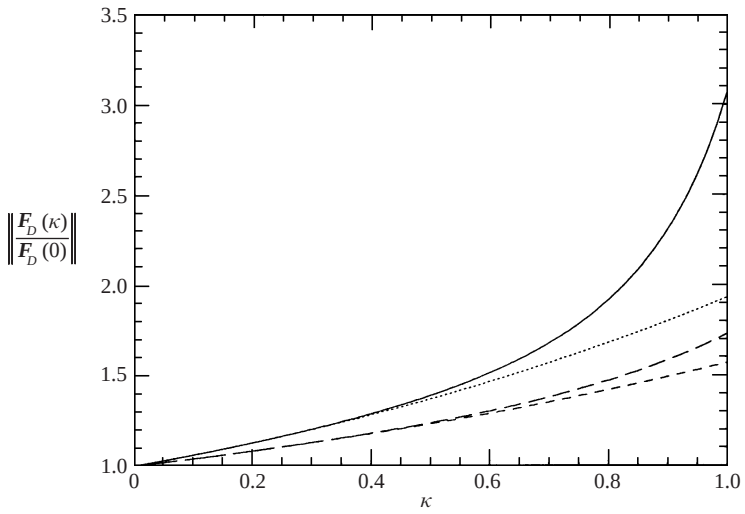

FIGURE 3. The wall-induced correction to the drag: – – –, $\lambda = 0$, equation (13a); · · · · · ·, $\lambda \to \infty$, equation (13b); — —, $\lambda = 0$, equation (16a); ——, $\lambda \to \infty$, equation (16b).

with

$$\boldsymbol{U}_Q = (\tfrac{1}{2}[K_{SO}(I_{C2} + I_{C3}) + D_\mu(I_{DC2} + I_{DC3})]x_1^2 + [K_{SO}I_{Q2} + D_\mu I_{DQ2}]x_2^2 + K_{SO}I_{Q3}x_3^2)\boldsymbol{e}_1 - [K_{SO}I_{C2} + D_\mu I_{DC2}]x_1x_2\boldsymbol{e}_2 - [K_{SO}I_{C3} + D_\mu I_{DC3}]x_1x_3\boldsymbol{e}_3 + O(\kappa^6). \tag{15c}$$

Here $\boldsymbol{T}_3$ and $\tilde{\boldsymbol{T}}_3$ denote the various terms due to the quadratic flow $\boldsymbol{U}_Q$ (except the stokeslet and the associated dipole, which are explicitly taken into account in K_{SD}), and $\boldsymbol{T}_4, \tilde{\boldsymbol{T}}_4, \boldsymbol{T}_5$ and $\tilde{\boldsymbol{T}}_5$ are the $O(\kappa^4)$ and $O(\kappa^5)$ terms that induce mode-4 and mode-5 deformations. In view of the amount of algebraic manipulations required and of the expected smallness of the associated deformations, we do not calculate these contributions explicitly. The numerical prefactors K_{SD}, K_{SS}, K_R and K_{SO} involved in (15a)–(15c) are given in Appendix B.

Multiplying K_{SD} by $-4\pi R_\mu V_{B1}^{(0)}$ yields the drag force on the particle, correct up to $O(\kappa^5)$. In the case of an inviscid bubble, we obtain

$$\boldsymbol{F}_D \approx -4\pi V_{B1}^{(0)} \left[1 - \tfrac{3}{8}\kappa - \tfrac{3}{64}\kappa^4\right]^{-1} \boldsymbol{e}_1. \tag{16a}$$

Similarly, we have for a very viscous drop or a rigid sphere

$$\boldsymbol{F}_D \approx -6\pi V_{B1}^{(0)} \left[1 - \tfrac{9}{16}\kappa + \tfrac{1}{8}\kappa^3 - \tfrac{45}{256}\kappa^4 - \tfrac{1}{16}\kappa^5\right]^{-1} \boldsymbol{e}_1, \tag{16b}$$

which is Faxén's well-known result (Happel & Brenner 1973, p. 327). According to the detailed measurements of Ambari, Gauthier–Manuel & Guyon (1983), the drag is very accurately predicted by (16) down to separations as small as $\kappa^{-1} \approx 1.01$. Having recovered Faxén's result as a particular case make us confident that the expression (B 5) for K_{SD} and the numerical coefficients it involves are correct whatever λ. The $O(\kappa^3)$ and $O(\kappa^5)$ approximations of the drag force corresponding to the two limits $\lambda = 0$ and $\lambda \to \infty$ are plotted in figure 3. It is seen that they do not differ much from each other whatever κ for an inviscid bubble. In contrast, in the limit of a very viscous drop, (16b) is found to agree closely with (13b) for $\kappa \leqslant 0.6$ but not for smaller

separations, and the difference between the two approximations is more than 60% for $\kappa \to 1$.

According to (15b), the fluid inside the drop has an average rotation rate $\Omega = \boldsymbol{\Omega}\cdot\boldsymbol{e}_2$ proportional to the prefactor K_R. In the limit of an inviscid bubble, (B 3) yields

$$\Omega = -\tfrac{3}{128}\kappa^5 V_{B1}^{(0)} + O(\kappa^6). \tag{17a}$$

However, this rotation is immaterial since it affects only the surface of the bubble. For a rigid sphere or a very viscous drop we recover Faxén's result

$$\Omega = \tfrac{3}{32}\kappa^4\left(1 - \tfrac{3}{8}\kappa\right) V_{B1}^{(0)} + O(\kappa^6). \tag{17b}$$

Interestingly the sign of Ω is different in the two limits considered above. Consequently, for a low enough viscosity ratio, there exists a distance from the wall at which the fluid inside the drop does not rotate at all. Moreover the fact that the sign of Ω changes with the viscosity ratio λ indicates that the origin of the near-wall rotation is quite subtle in the sense that its sign is not determined entirely by the wall but also depends on the mobility of the suspending fluid at the drop surface.

To obtain the new approximation of the deformation, we just have to note that the prefactor $I_S(1 - I_D)$ in (8a)–(10a) has been replaced by K_{SS} in (15a) while the prefactors of the quadratic terms in (7) have been replaced by those of (15c). Using (B 2), this yields immediately the improved approximation of the deformation as

$$f^{(\delta)} = V_{B1}^{(0)}\left\{\frac{16+19\lambda}{4(1+\lambda)}K_{SS}\frac{x_1x_3}{r^2} + \frac{10+11\lambda}{8(1+\lambda)}\frac{x_1}{r}\left[\frac{K_2+K_3}{2}\left(\frac{x_1^2}{r^2} - \tfrac{3}{5}\right)\right.\right.$$
$$\left.\left. + K_2\left(\frac{x_2^2}{r^2} - \tfrac{1}{5}\right) + K_3\left(\frac{x_3^2}{r^2} - \tfrac{1}{5}\right)\right]\right\} + M_4 + M_5 + O(\kappa^6), \tag{18}$$

with $K_2 = K_{SO}(I_{Q2} - I_{C2}) + D_\mu(I_{DQ2} - I_{DC2})$, $K_3 = K_{SO}(I_{Q3} - I_{C3}) - D_\mu I_{DC3}$ (see (A 3b)–(A 4b)), M_4 and M_5 denoting fourth- and fifth-order deformations produced by terms $\boldsymbol{T}_4$, $\tilde{\boldsymbol{T}}_4$, $\boldsymbol{T}_5$ and $\tilde{\boldsymbol{T}}_5$ of (15a, b). In the limit of an inviscid bubble, (18) shows that the mode-2 contribution $f_2^{(\delta)}$ to $f^{(\delta)}$ is

$$f_2^{(\delta)} = \tfrac{3}{8}V_{B1}^{(0)}\kappa^2\left\{\left[1 + \tfrac{3}{8}\kappa\left(1 + \tfrac{3}{8}\kappa + \tfrac{73}{64}\kappa^2\right)\right]\sin 2\theta \sin\varphi, \right. \tag{19a}$$

while in the limit of a very viscous drop we have

$$f_2^{(\delta)} = \tfrac{171}{256}V_{B1}^{(0)}\kappa^2\left\{\left[1 + \tfrac{9}{16}\kappa\left(1 - \tfrac{47}{144}\kappa + \tfrac{9227}{6912}\kappa^2\right)\right]\sin 2\theta \sin\varphi. \right. \tag{19b}$$

Predictions of (14b) (for mode 2) and (19) are compared in figure 4 for the particular orientation $\theta = \pi/4$, $\varphi = \pi/2$. This comparison indicates that the strength of mode 2 is significantly different in the two approximations. Equations (19) predict about 40% more deformation that (14b) for $\kappa \to 1$ and the difference is still about 8% for $\kappa = 1/2$. Most of the difference is due to the factor I_{SS} in the prefactor K_{SS}, i.e. to the stresslet induced by the first reflection of the stresslet present in the velocity field ${}_3\boldsymbol{U}^{(0)}$. We note that the dipole tends to reduce the deformation, since all contributions multiplied by D_μ in (B 2) are negative. Takemura *et al.* (2002) compared the prediction (19a) with a detailed experimental determination of the mode f_2 for millimetric air bubbles. They found a very good agreement over the whole range of separations covered by their experiments, i.e. $\kappa \leqslant 0.6$ (see their figure 14).

3.4. *Linear shear flow*

The results established above may be used to obtain, with very little additional effort, the $O(\kappa^3)$-approximation of the drag force and deformation of a buoyant drop moving

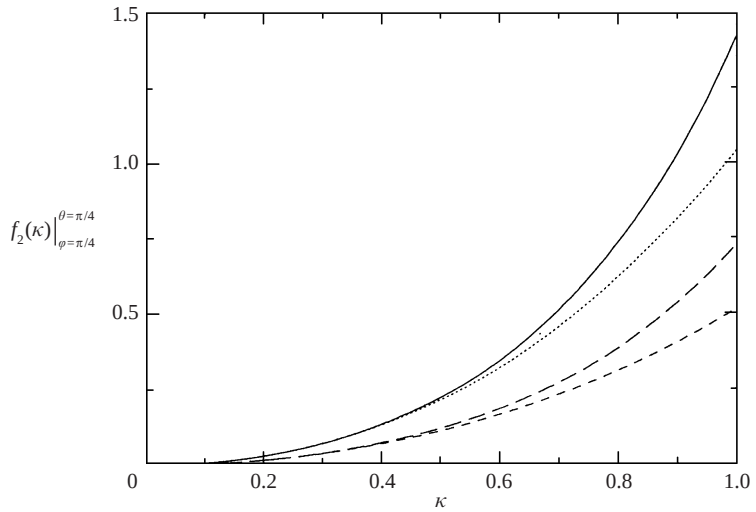

FIGURE 4. Evolution of the mode-2 deformation with the distance to the wall: – – –, $\lambda = 0$, equation (14b); · · · · · ·, $\lambda \to \infty$, equation (14b); ——, $\lambda = 0$, equation (19a); ——, $\lambda \to \infty$, equation (19b).

in a linear shear flow bounded by a single wall. For this purpose, let the undisturbed dimensionless velocity field be defined by†

$$\boldsymbol{U}_\infty(x_3) = \alpha\left(x_3 + \frac{1}{\kappa}\right)\boldsymbol{e}_1. \tag{20}$$

Then the slip velocity between the drop and the undisturbed flow is $\boldsymbol{V}_S = \boldsymbol{V}_B - (\alpha/\kappa)\boldsymbol{e}_1$, and the effects of this slip velocity are obtained by replacing $\boldsymbol{V}_B$ (resp. $V_{B1}^{(0)}$) by $\boldsymbol{V}_S$ (resp. $V_{S1}^{(0)} = V_{B1}^{(0)} - \alpha/\kappa$) in all equations of §§ 3.1 and 3.2. Using (8a, b), we find immediately that the contribution of the shear to be added to the unbounded solution (5a, b) is

$${}_1\boldsymbol{U}_\alpha^{(0)} = \alpha\left\{x_3\boldsymbol{e}_1 - \left[R_S\frac{x_1x_3\boldsymbol{x}}{r^5} + 2D_\mu\left(\frac{x_3\boldsymbol{e}_1}{r^5} + \frac{x_1\boldsymbol{e}_3}{r^5} - 5\frac{x_1x_3\boldsymbol{x}}{r^7}\right)\right]\right\}, \tag{21a}$$

$${}_1\tilde{\boldsymbol{U}}_\alpha^{(0)} = \frac{\alpha}{2}\{(x_3\boldsymbol{e}_1 - x_1\boldsymbol{e}_3) + M_\mu[(5r^2-3)(x_3\boldsymbol{e}_1 + x_1\boldsymbol{e}_3) - 4x_1x_3\boldsymbol{x}]\}. \tag{21b}$$

To obtain the complete solution at $O(\kappa^3)$ we only need to consider the reflection of the stresslet since the reflection of the quadrupole produces only terms of $O(\kappa^4)$. Using (A 5) and (15a, b) we find that this reflection induces the velocity fields (to be added to (8a, b))

$$\begin{aligned}\sum_{k=2}^{k=5}{}_k\boldsymbol{U}_\alpha^{(0)} = \alpha R_S\Bigg\{&I_{SD}(1-I_D)\left[-\boldsymbol{e}_1 + \frac{R_\mu}{2}\left(\frac{\boldsymbol{e}_1}{r} + \frac{x_1\boldsymbol{x}}{r^3}\right) + D_\mu\left(\frac{\boldsymbol{e}_1}{r^3} - 3\frac{x_1\boldsymbol{x}}{r^5}\right)\right]\\ &-I_{SR}(x_3\boldsymbol{e}_1 - x_1\boldsymbol{e}_3) + 2I_{SS}\Bigg[-\tfrac{1}{2}(x_3\boldsymbol{e}_1 + x_1\boldsymbol{e}_3) + R_S\frac{x_1x_3\boldsymbol{x}}{r^5}\\ &+2D_\mu\left(\frac{x_3\boldsymbol{e}_1}{r^5} + \frac{x_1\boldsymbol{e}_3}{r^5} - 5\frac{x_1x_3\boldsymbol{x}}{r^7}\right)\Bigg]\Bigg\} + O(\kappa^4),\end{aligned} \tag{22a}$$

† Given the scaling defined in § 2, the dimensional shear rate is then $\dot{\gamma} = \alpha\rho|1-\bar{\rho}|Rg/\mu$.

$$\sum_{k=3,5} {}_k\tilde{\boldsymbol{U}}_{\alpha}^{(0)} = \alpha R_S\{M_\mu I_{SD}(1-I_D)[(1-2r^2)\boldsymbol{e}_1 + x_1\boldsymbol{x}] - I_{SR}(x_3\boldsymbol{e}_1 - x_1\boldsymbol{e}_3)$$
$$-M_\mu I_{SS}[(5r^2-3)(x_3\boldsymbol{e}_1 + x_1\boldsymbol{e}_3) - 4x_1x_3\boldsymbol{x}]\} + O(\kappa^4). \tag{22b}$$

Equation (22a) shows that the shear induces a stokeslet of strength $\alpha R_S R_\mu I_{SD}(1-I_D)$. Combining this result with (12), we see that the drag force experienced by the drop is now

$$\boldsymbol{F}_D = -4\pi R_\mu \left\{ V_{S1}^{(0)} \left(1 + \tfrac{3}{8}R_\mu\kappa + \tfrac{9}{64}R_\mu^2\kappa^2 + \left(\tfrac{27}{512}R_\mu^3 - \frac{D_\mu}{2}\right)\kappa^3\right) \right.$$
$$\left. + \frac{\alpha}{8}R_S\kappa^2\left(1 + \tfrac{3}{8}R_\mu\kappa\right)\right\}\boldsymbol{e}_1 + O(\kappa^4). \tag{23a}$$

In the limit $\lambda \to \infty$ the shear increases the drag by $\frac{15}{8}\pi\alpha\kappa^2(1 + \frac{9}{16}\kappa)$, a prediction in agreement with that of Halow & Wills (1970). From (23a) one deduces that in the case of a neutrally buoyant drop the condition $\boldsymbol{F}_D = \boldsymbol{0}$ yields the slip velocity

$$V_{S1}^{(0)} = -\frac{\alpha}{8}R_S\kappa^2 + O(\kappa^4). \tag{23b}$$

Therefore the drop lags slightly behind the fluid.† From (21)–(22) we also conclude that the fluid inside the drop rotates at an average rate $\Omega = \frac{1}{2}\alpha(1 - \frac{1}{8}R_S\kappa^3)$ and that the mode-2 contribution to the deformation of the drop is

$$f_2^{(\delta)} = \frac{16+19\lambda}{8(1+\lambda)}\left[\alpha\left(1 + \tfrac{3}{8}R_S\kappa^3\right) + \tfrac{3}{8}V_{S1}^{(0)}\kappa^2 R_\mu\left(1 + \tfrac{3}{8}R_\mu\kappa\right) + O(\kappa^4)\right]\frac{x_1x_3}{r^2}. \tag{24}$$

The deformation is aligned with the imposed strain and its leading-order expression is of course identical to that found by Taylor (1932, 1934) in an unbounded linear shear flow. The dominant contribution due to the wall is still that determined in (14a) if $V_{S1}^{(0)}$ is $O(1)$; in contrast, if the drop is neutrally buoyant the contribution of the slip velocity becomes of $O(\kappa^4)$ and the leading effect of the wall occurs through the factor $\frac{3}{8}\alpha R_S\kappa^3$.

4. The complementary problem

Instead of solving completely the $O(G)$ and $O(\delta)$ problems corresponding to (4a, b), we shall follow the technique used by Ho & Leal (1974) and Chan & Leal (1979), i.e. we shall determine the migration velocity by taking advantage of a suitable form of the reciprocal theorem. In order to do so, we first need to solve the 'complementary' problem of *a spherical* drop moving perpendicularly to the wall with a unit velocity $\boldsymbol{e}_3$ under *creeping* flow conditions. The governing equations of the problem are

$$\left.\begin{array}{l} \nabla\cdot\boldsymbol{u} = 0, \quad \nabla\cdot\boldsymbol{\sigma} = \boldsymbol{0}, \\ \nabla\cdot\tilde{\boldsymbol{u}} = 0, \quad \nabla\cdot\tilde{\boldsymbol{\sigma}} = \boldsymbol{0}, \\ \boldsymbol{u} = -\boldsymbol{e}_3 \quad \text{for} \quad x_3 = -1/\kappa, \\ \boldsymbol{u} \to -\boldsymbol{e}_3 \quad \text{for} \quad r \to \infty, \\ \left.\begin{array}{l} \boldsymbol{u}\cdot\boldsymbol{e}_r = \tilde{\boldsymbol{u}}\cdot\boldsymbol{e}_r = 0 \\ \boldsymbol{e}_r\times\boldsymbol{u} = \boldsymbol{e}_r\times\tilde{\boldsymbol{u}} \\ \boldsymbol{e}_r\times(\boldsymbol{\sigma}\cdot\boldsymbol{e}_r) = \lambda\boldsymbol{e}_r\times(\tilde{\boldsymbol{\sigma}}\cdot\boldsymbol{e}_r) \end{array}\right\} \quad \text{for} \quad r = 1, \end{array}\right\} \tag{25}$$

† For a neutrally or an almost-neutrally buoyant drop, the scaling defined in § 2 is inappropriate; the correct velocity scale must then be based on the shear velocity, i.e. the velocity difference over one drop radius. With this re-scaling, the dimensionless shear rate α becomes $\alpha \equiv 1$.

where $\boldsymbol{\sigma} = -p\boldsymbol{I} + \nabla\boldsymbol{u} + \nabla^T\boldsymbol{u}$ and $\tilde{\boldsymbol{\sigma}} = -\tilde{p}\boldsymbol{I} + \nabla\tilde{\boldsymbol{u}} + \nabla^T\tilde{\boldsymbol{u}}$ are the corresponding stress tensors and p and $\tilde{p}$ are the associated pressures. Note that the normal stresses obtained by solving (25) will generally be discontinuous at the drop surface. The solution in unbounded flow is obviously

$$ {}_1\boldsymbol{u} = -\boldsymbol{e}_3 + \frac{R_\mu}{2}\left(\frac{\boldsymbol{e}_3}{r} + \frac{x_3\boldsymbol{x}}{r^3}\right) + D_\mu\left(\frac{\boldsymbol{e}_3}{r^3} - 3\frac{x_3\boldsymbol{x}}{r^5}\right), \tag{26a} $$

$$ {}_1\tilde{\boldsymbol{u}}^{(0)} = M_\mu[(1-2r^2)\boldsymbol{e}_3 + x_3\boldsymbol{x}]. \tag{26b} $$

The reflection of the stokeslet and dipole involved in (26a) is obtained by using techniques similar to those employed before; the corresponding results are given by (A 6)–(A 7) of Appendix A. Expanding the first reflection of the complete unbounded solution in the vicinity of the drop, we then find

$$ \begin{aligned} {}_2\boldsymbol{u}(\kappa r \ll 1) = {} & (J_D + D_\mu J_0)\boldsymbol{e}_3 + J_S(\boldsymbol{x} - 3x_3\boldsymbol{e}_3) \\ & -J_C(x_1x_3\boldsymbol{e}_1 + x_2x_3\boldsymbol{e}_2) + (J_Cx_3^2 + J_Q(x_1^2 + x_2^2))\boldsymbol{e}_3 + O(\kappa^4), \end{aligned} \tag{27} $$

where $J_D = R_\mu J'_D$, etc. the primed quantities and the prefactor J_0 being given by (A 6b) and (A 7b), respectively. To determine $\boldsymbol{u}$ and $\tilde{\boldsymbol{u}}$ up to terms of $O(\kappa^3)$ we employ the same procedures as in the derivation of (14a,b). We then obtain

$$ \begin{aligned} \sum_{k=3}^{7} {}_k\boldsymbol{u} = {} & (-J_D + J_D^2 - J_D^3 - D_\mu J_0)\left[\frac{R_\mu}{2}\left(\frac{\boldsymbol{e}_3}{r} + \frac{x_3\boldsymbol{x}}{r^3}\right) + D_\mu\left(\frac{\boldsymbol{e}_3}{r^3} - 3\frac{x_3\boldsymbol{x}}{r^5}\right)\right] \\ & -J_S(1-J_D)\left[R_S\left(\frac{\boldsymbol{x}}{r^3} - 3\frac{x_3^2\boldsymbol{x}}{r^5}\right) - 6D_\mu\left(\frac{\boldsymbol{x}}{r^5} + 2\frac{x_3\boldsymbol{e}_3}{r^5} - 5\frac{x_3^2\boldsymbol{x}}{r^7}\right)\right] \\ & -J_D^2(1-J_D)\boldsymbol{e}_3 - J_SJ_D(\boldsymbol{x} - 3x_3\boldsymbol{e}_3) + \boldsymbol{v}_3 + O(\kappa^4), \end{aligned} \tag{28a} $$

$$ \begin{aligned} \sum_{k=2}^{k=7} {}_k\tilde{\boldsymbol{u}}^{(0)} = {} & M_\mu\{(-J_D + J_D^2 - J_D^3 - D_\mu J_0)[(1-2r^2)\boldsymbol{e}_3 + x_3\boldsymbol{x}] \\ & +3J_S(1-J_D)[(r^2 + 2x_3^2 - 1)\boldsymbol{x} + (3-5r^2)x_3\boldsymbol{e}_3] + \tilde{\boldsymbol{v}}_3\} + O(\kappa^4), \end{aligned} \tag{28b} $$

where $\boldsymbol{v}_3$ and $\tilde{\boldsymbol{v}}_3$ denote the $O(\kappa^3)$ terms due to the quadratic contribution in ${}_2\boldsymbol{u}$. Again $\boldsymbol{v}_3$ includes a stokeslet of strength $-R_\mu D_\mu K_{DC}$, with $K_{DC} = 2(J'_C + 2J'_Q) = \kappa^3$. Applying Faxén's formula to the sum of (26a), (27) and (28a), the drag force on the drop is found to be

$$ \boldsymbol{F}_{DC} = -4\pi R_\mu\left(\sum_{n=0}^{3}(-1)^nJ_D^n - D_\mu(J_0 + K_{DC})\right)\boldsymbol{e}_3 + O(\kappa^4). \tag{29} $$

In the case of an inviscid bubble, (29) yields

$$ \boldsymbol{F}_{DC} = -4\pi\left(1 + \tfrac{3}{4}\kappa + \tfrac{9}{16}\kappa^2 + \tfrac{27}{64}\kappa^3\right)\boldsymbol{e}_3 + O(\kappa^4), \tag{30a} $$

whereas for a solid sphere or a very viscous drop it becomes

$$ \boldsymbol{F}_{DC} = -6\pi\left(1 + \tfrac{9}{8}\kappa + \tfrac{81}{64}\kappa^2 + \tfrac{473}{512}\kappa^3\right)\boldsymbol{e}_3 + O(\kappa^4). \tag{30b} $$

The latter result agrees with that of Wakiya, reported by Happel & Brenner (1973, p. 330) (see § 7 for a discussion on the validity of (29)–(30)). Again we see that the presence of the wall increases the drag force. Comparing with (13a,b) reveals that this increase is larger than in the situation where the drop moves parallel to the wall (the

leading-order term in (30) is twice that in (13)). This may be readily understood by noting that the flow about a particle moving perpendicular to the wall involves highly curved streamlines, as they are perpendicular to the wall near the symmetry axis of the motion and parallel to it near the wall. Hence high strain rates are generated near the wall, thus increasing dramatically the force required to move the drop when it comes close to the wall.

We note in passing that if we provisionally allow the drop to deform (i.e. we add the normal stress balance to the set of equations (25)), the corresponding deformation may easily be predicted from (27)–(28). To obtain this deformation, $f_\perp$ say, we evaluate the normal stresses produced by the linear part of ${}_2\boldsymbol{u}$ and the associated singularities in (28*a*, *b*) and we note that the quadratic terms in (27) have the same structure as in (7) up to a rotation of $-\pi/2$ about the x_2-axis. Hence the mode-3 deformation may be directly deduced from (14*a*) provided x_3 and $\boldsymbol{e}_3$ (resp. x_1 and $\boldsymbol{e}_1$) are replaced by x_1 and $\boldsymbol{e}_1$ (resp. $-x_3$ and $-\boldsymbol{e}_3$), and I_{Q2} and I_{Q3} (resp. I_{C2} and I_{C3}) are replaced by $-J_Q$ (resp. $-J_C$). For a unit translation velocity and unit Bond number, the result is then

$$f_\perp = \tfrac{3}{8}R_\mu\kappa^2\left[\frac{16+19\lambda}{16(1+\lambda)}\left(1+\tfrac{3}{4}R_\mu\kappa\right)\left(3\frac{x_3^2}{r^2}-1\right)\right.$$
$$\left.+\tfrac{3}{8}\kappa\frac{10+11\lambda}{10(1+\lambda)}\frac{x_3}{r}\left(5\frac{x_3^2}{r^2}-3\right)\right]+O(\kappa^4). \tag{31}$$

As the strain rate near the drop has the same magnitude as in the case of a motion parallel to the wall, the leading-order term in (31) is again of $O(\kappa^2)$; obviously the drop is now axisymmetric about the x_3-axis. A drop receding from the wall is elongated along this axis and the mode-3 contribution has a maximum at the front pole ($x_3 > 0$). If the velocity of the drop is reversed, so that it now goes towards the wall, all signs are changed in (31), i.e. the drop is now flattened along the x_3-direction and the mode-3 contribution has a maximum at the pole located close to the wall ($x_3 < 0$). These two situations are illustrated in figure 5 for two different values of κ; note that when the drop moves towards the wall, the combination of the two modes taken into account in (31) may lead to a dimple at the rear of the drop for large enough κ and λ. Predictions of (31) may be compared with the analytical solution obtained by Chervenivanova & Zapryanov (1985) using bispherical coordinates, or with the numerical solution of Ascoli, Dandy & Leal (1990) obtained by solving Stokes equation with fully nonlinear boundary conditions at the drop surface for the case of a drop falling towards a horizontal wall under the effect of buoyancy. According to figure 1 of the former reference and to figure 3 of the latter one, predictions of (31) agree with previous findings provided the distance to the wall is large enough for the present analysis to be applicable, i.e. $\kappa \leqslant 1/2$ approximately. For smaller separations (typically $\kappa \geqslant 2/3$), a dimple appears between the drop and the wall in the exact solution; this feature is not captured by the low-order description (31), which indicates that it results either from a higher-order mode of deformation or from a reversal of the sign of mode 3 through higher-order corrections (i.e. $O(\kappa^n)$ with $n > 3$) to its amplitude.

5. The deformation-induced migration

To obtain the lift force on the drop we shall follow Ho & Leal (1974) and Chan & Leal (1979) and make use of the reciprocal theorem. However, inertia was considered

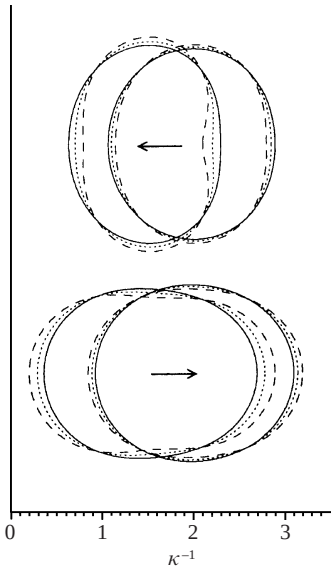

FIGURE 5. The shape of a deformed drop moving perpendicular to the wall as predicted by equation (31) for $\kappa = 0.5$ and 0.67 (the Bond number is arbitrarily set to 0.33): ——, $\lambda = 0$; · · · · · ·, $\lambda = 1$; – – –, $\lambda \to \infty$.

only for a rigid sphere in these works and buoyancy was neglected. Consequently, we present a brief outline of the derivation of the reciprocal theorem for the more general situation considered here. For this purpose we start from the momentum balance outside and inside the drop as given by (2*a*) and (25), and combine the properties of the solution $(\boldsymbol{U}, \boldsymbol{\Sigma})$ obtained in § 3 with those of the complementary solution $(\boldsymbol{u}, \boldsymbol{\sigma})$ determined in § 4. Using the divergence theorem, integrating over the corresponding fluid volume and taking into account the boundary conditions on the wall and the behaviour of $\boldsymbol{U}, \boldsymbol{u}, \boldsymbol{\Sigma}$, and $\boldsymbol{\sigma}$ in the far field we obtain

$$\int_{A_B} [(\boldsymbol{U} + \boldsymbol{V}_B) \cdot \boldsymbol{\sigma} - (\boldsymbol{u} + \boldsymbol{e}_3) \cdot \boldsymbol{\Sigma}] \cdot \boldsymbol{n} \, \mathrm{d}S = G \int_{V_F} (\boldsymbol{u} + \boldsymbol{e}_3) \cdot (\boldsymbol{U} \cdot \nabla) \boldsymbol{U} \, \mathrm{d}V, \tag{32a}$$

$$\lambda \int_{A_B} (\tilde{\boldsymbol{u}} \cdot \tilde{\boldsymbol{\Sigma}} - \tilde{\boldsymbol{U}} \cdot \tilde{\boldsymbol{\sigma}}) \cdot \boldsymbol{n} \, \mathrm{d}S = \bar{\rho} G \int_{V_B} \tilde{\boldsymbol{u}} \cdot (\tilde{\boldsymbol{U}} \cdot \nabla) \tilde{\boldsymbol{U}} \, \mathrm{d}V, \tag{32b}$$

where A_B (resp. V_B) denotes the surface (resp. volume) of the drop, $\boldsymbol{n}$ is the unit normal directed into the suspending fluid and V_F is the entire volume of fluid surrounding the drop. Since $\int_{A_B} \boldsymbol{\Sigma} \cdot \boldsymbol{n} \, \mathrm{d}S$ just balances the net buoyancy force (see (2*b*)), its dot product with $\boldsymbol{e}_3$ is zero. Hence (32*a*, *b*) may be added to obtain the transverse component of the drop velocity, $V_{B3} = \boldsymbol{V}_B \cdot \boldsymbol{e}_3$, in the form

$$(\boldsymbol{F}_{DC} \cdot \boldsymbol{e}_3) V_{B3} = G \int_{V_F} (\boldsymbol{u} + \boldsymbol{e}_3) \cdot (\boldsymbol{U} \cdot \nabla \boldsymbol{U}) \, \mathrm{d}V + \bar{\rho} G \int_{V_B} \tilde{\boldsymbol{u}} \cdot (\tilde{\boldsymbol{U}} \cdot \nabla \tilde{\boldsymbol{U}}) \, \mathrm{d}V$$
$$+ \int_{A_B} (\boldsymbol{u} \cdot \boldsymbol{\Sigma} - \lambda \tilde{\boldsymbol{u}} \cdot \tilde{\boldsymbol{\Sigma}}) \cdot \boldsymbol{n} \, \mathrm{d}S - \int_{A_B} (\boldsymbol{U} \cdot \boldsymbol{\sigma} - \lambda \tilde{\boldsymbol{U}} \cdot \tilde{\boldsymbol{\sigma}}) \cdot \boldsymbol{n} \, \mathrm{d}S, \tag{33}$$

with $\boldsymbol{F}_{DC} \cdot \boldsymbol{e}_3$ given by (29). Equation (33) may now be expanded in powers of the Galileo number G and Bond number δ. Taking into account the boundary conditions at $r = 1$ in (3) and (25), it turns out that the two surface integrals in (33) are identically

zero at $O(G)$. We are then left with

$$(\boldsymbol{F}_{DC}\cdot\boldsymbol{e}_3)V_{B3}^{(G)}=\int_{V_F}(\boldsymbol{u}+\boldsymbol{e}_3)\cdot(\boldsymbol{U}^{(0)}\cdot\nabla)\boldsymbol{U}^{(0)}\,\mathrm{d}V+\bar{\rho}\int_{V_B}\tilde{\boldsymbol{u}}\cdot(\tilde{\boldsymbol{U}}^{(0)}\cdot\nabla\tilde{\boldsymbol{U}}^{(0)})\,\mathrm{d}V. \tag{34a}$$

Similarly, the $O(\delta)$ approximations is

$$\begin{aligned}(\boldsymbol{F}_{DC}\cdot\boldsymbol{e}_3)V_{B3}^{(\delta)}=&-\int_{A_{B0}}\boldsymbol{U}^{(\delta)}\cdot(\boldsymbol{\sigma}-\lambda\tilde{\boldsymbol{\sigma}})\cdot\boldsymbol{e}_r\,\mathrm{d}S+\int_{A_{B0}}\boldsymbol{u}\cdot(\boldsymbol{\Sigma}^{(\delta)}-\lambda\tilde{\boldsymbol{\Sigma}}^{(\delta)})\cdot\boldsymbol{e}_r\,\mathrm{d}S\\&-\lambda\int_{A_{B0}}(\boldsymbol{U}^{(\delta)}-\tilde{\boldsymbol{U}}^{(\delta)})\cdot\tilde{\boldsymbol{\sigma}}\cdot\boldsymbol{e}_r\,\mathrm{d}S,\end{aligned} \tag{34b}$$

where A_{B0} denotes the undeformed drop surface. We note that in the limit $\lambda\to\infty$, $\tilde{\boldsymbol{U}}^{(0)}$ and $\tilde{\boldsymbol{u}}$ necessarily reduce to solid body rotations. However, the rotation of the drop is zero in the complementary problem, owing to the symmetry about the x_3-axis. Consequently the last term on the right-hand side of (34a) vanishes, and we recover the expression for the inertial migration velocity established for a rigid particle by Ho & Leal (1974).

5.1. *The deformation-induced lift force*

The right-hand side of (34b) may now be expressed in terms of known quantities by using the kinematic and dynamic boundary conditions as they appear in (3a) and (4b). This yields, in agreement with (6.6) of Chan & Leal (1979),

$$\begin{aligned}(\boldsymbol{F}_{DC}\cdot\boldsymbol{e}_3)V_{B3}^{(\delta)}=&\int_{A_{B0}}\{f^{(\delta)}(\partial\boldsymbol{U}^{(0)}/\partial r)\cdot\boldsymbol{e}_r-\boldsymbol{U}^{(0)}\cdot\nabla f^{(\delta)}\}\boldsymbol{e}_r\cdot(\boldsymbol{\sigma}-\lambda\tilde{\boldsymbol{\sigma}})\cdot\boldsymbol{e}_r\,\mathrm{d}S\\&+\int_{A_{B0}}\left\{\boldsymbol{u}\cdot(\boldsymbol{\Sigma}^{(0)}-\lambda\tilde{\boldsymbol{\Sigma}}^{(0)})\cdot\nabla f^{(\delta)}-f^{(\delta)}\boldsymbol{u}\cdot\frac{\partial}{\partial r}(\boldsymbol{\Sigma}^{(0)}-\lambda\tilde{\boldsymbol{\Sigma}}^{(0)})\cdot\boldsymbol{e}_r\right\}\mathrm{d}S\\&+\int_{A_{B0}}\boldsymbol{u}\cdot\nabla f^{(\delta)}(\nabla^2 f^{(\delta)}+2f^{(\delta)})\,\mathrm{d}S+\lambda\int_{A_{B0}}f^{(\delta)}\frac{\partial}{\partial r}(\boldsymbol{U}^{(0)}-\tilde{\boldsymbol{U}}^{(0)})\cdot\tilde{\boldsymbol{\sigma}}\cdot\boldsymbol{e}_r\,\mathrm{d}S.\end{aligned} \tag{35}$$

Since the left-hand side of (35) is just the horizontal drag force acting on the drop, the force balance (4c) implies that the right-hand side is the opposite of the deformation-induced lift force. Examination of the various quantities involved in the integrands up to $O(\kappa^3)$ shows that the deformation induced by the quadratic part of ${}_2\boldsymbol{U}^{(0)}$ in (7) does not contribute to the migration at this order of approximation, owing to its symmetry with respect to the plane $x_3=0$. Consequently, the migration evaluated below is entirely due to the mode-2 deformation (note that the mode 4 formally included in (18) would contribute to the migration at $O(\kappa^4)$). Moreover, since the leading-order deformation is $O(\kappa^2)$ (see (14a)), only terms of $O(1)$ and $O(\kappa)$ need to be considered in the velocity and stress fields. This means that only the stokeslet and associated singularities in the unbounded solution (5) and (26) contribute to this approximation of the migration. Based on these remarks, the integrands involved in (35) may be evaluated. Performing integrations we finally obtain

$$\begin{aligned}\boldsymbol{F}_M^{(\delta)}&\approx 4\pi R_\mu\left(1+\tfrac{3}{4}R_\mu\kappa\right)V_{B3}^{(\delta)}\boldsymbol{e}_3\\&=\frac{3\pi}{320}\frac{16+19\lambda}{(1+\lambda)^3}R_\mu(2-10\lambda+3\lambda^2)\kappa^2\left(1+\tfrac{3}{2}R_\mu\kappa\right)(V_{B1}^{(0)})^2\boldsymbol{e}_3+O(\kappa^4).\end{aligned} \tag{36}$$

Given the presence of the factor κ^2 in (36), we see that $|V_{B3}^{(\delta)}|$ decreases inversely with the square of the separation distance to the wall. An interesting feature of (36) is that

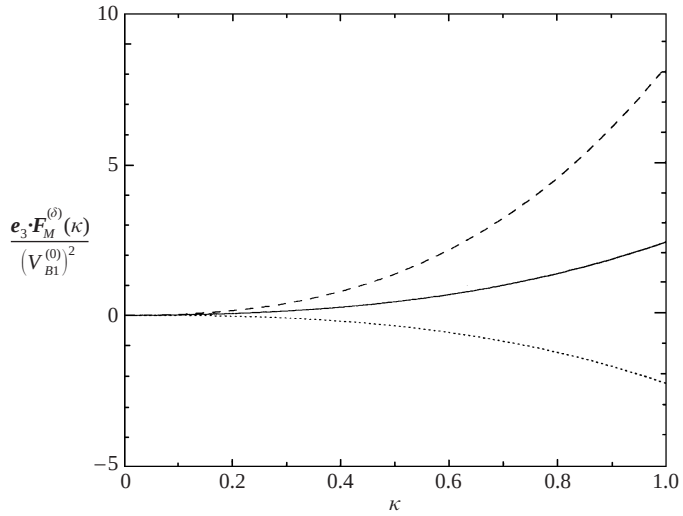

FIGURE 6. The normalized deformation-induced lift force as a function of the distance to the wall, as predicted by equation (37) (fluid at rest at infinity): ——, $\lambda = 0$; · · · · · ·, $\lambda = 1$; – – –, $\lambda \to \infty$.

it predicts that the direction of the migration depends on the viscosity ratio λ. More precisely the drop is found to migrate *away* from the wall for $\lambda < (5 - 19^{1/2})/3 \approx 0.21$ and $\lambda > (5 + 19^{1/2})/3 \approx 3.12$, and *towards* it when λ lies between the foregoing two limits. We are not aware of measurements performed in this intermediate range of λ that could confirm or contradict this prediction. Nevertheless we have carefully checked the above result and we are confident that it is correct. We also note that Chan & Leal (1979) found a similar feature for a drop migrating in a plane Poiseuille flow where they showed that the direction of the deformation-induced migration changes with λ and is towards the wall for $O(1)$-values of λ. That the deformation-induced migration experienced by an almost inviscid bubble rising in a quiescent liquid is directed away from the wall was clearly established experimentally by Takemura *et al.* (2002) (see their figure 12). However, inertia also contributed to the migration in their experiments, thus preventing a quantitative comparison with (36). In the limit of an inviscid bubble (36) yields

$$\boldsymbol{F}_M^{(\delta)} = \tfrac{3}{10}\pi\kappa^2\left(1 + \tfrac{3}{2}\kappa\right)(V_{B1}^{(0)})^2\boldsymbol{e}_3 + O(\kappa^4). \tag{37a}$$

In the opposite case of a very viscous drop, the above prediction becomes

$$\boldsymbol{F}_M^{(\delta)} = \tfrac{171}{320}\pi\kappa^2\left(1 + \tfrac{9}{4}\kappa\right)(V_{B1}^{(0)})^2\boldsymbol{e}_3 + O(\kappa^4), \tag{37b}$$

whereas for homoviscous fluids ($\lambda = 1$) it is

$$\boldsymbol{F}_M^{(\delta)} = \tfrac{105}{512}\pi\kappa^2\left(1 + \tfrac{15}{8}\kappa\right)(V_{B1}^{(0)})^2\boldsymbol{e}_3 + O(\kappa^4). \tag{37c}$$

Predictions of (37) are plotted in figure 6. Interestingly, the origin of each of the three terms in the coefficient $2 - 10\lambda + 3\lambda^2$ of (36) may be readily identified in (34*b*) and (35). The first of these terms (which yields the result (37*a*)) comes from the first integral on the right-hand side of (34*b*) and (35), and is due to the non-zero $O(\delta)$-normal velocity at $r = 1$. This term is proportional to the factor $R_\mu M_\mu$, i.e. to the product of the strength of the stokeslet in the unbounded solution (5*a*) and the mobility of the fluid inside the drop (5*b*). The quadratic term (which yields the result (37*b*)) comes from the last integral and is due to the $O(\delta)$-velocity jump at $r = 1$.

This term is proportional to the product of the strength of the dipole in (5*a*) by a linear combination of R_μ and D_μ. Finally, the linear term reponsible for the negative sign of the lift force for $O(1)$-viscosity ratios comes from the second integral and is due to the $O(\delta)$-jump of the tangential stresses at $r = 1$. This term is linearly proportional to $D_\mu M_\mu$, and then vanishes in the two limits $\lambda \to 0$ and $\lambda \to \infty$. This analysis show how subtle the mechanism of deformation-induced migration is. The migration occurs because two ingredients are present, i.e. the flow about the drop is asymmetric (here due to the presence of the wall), and deformation introduces irreversibility through the boundary conditions (see (4*b*)). The resulting migration is then proportional to the product of the slip velocity (here of $O(1)$) by the magnitude of the deformation (of $O(\kappa^2)$ in the present case). Nevertheless, drawing this general picture does not give any indication of the direction of the migration and we just saw that in general this direciton may change with the viscosity ratio, according to the relative strength of several different contributions to the boundary conditions.

The result (36) and those obtained in § 3.4 may be used to predict the $O(\kappa^2)$ approximation of the deformation-induced migration of a buoyant drop moving in a linear shear flow. For this purpose the strength of the mode-2 deformation given by (14*a*) must be replaced by that given in (24). Furthermore, since the deformation is now $O(1)$ instead of $O(\kappa^2)$, it is necessary to consider terms up to $O(\kappa^2)$ in the slip velocity determined in (23), i.e. the velocity $V_{B1}^{(0)}(1 + \frac{3}{8}R_\mu\kappa)$ must be replaced by $V_{S1}^{(0)}(1 + \frac{3}{8}R_\mu\kappa + \frac{9}{64}R_\mu^2\kappa^2) + \frac{\alpha}{8}R_S\kappa^2$. Inserting these values in (36) and evaluating the right-hand side of (35) for the velocity field given by (21*a*, *b*) finally yields

$$\boldsymbol{F}_M^{(\delta)} = \frac{\pi}{320}\frac{16+19\lambda}{(1+\lambda)^3}\left\{(2-10\lambda+3\lambda^2)\left[8\alpha V_{S1}^{(0)}\left(1+\tfrac{9}{8}R_\mu\kappa+\tfrac{63}{64}R_\mu^2\kappa^2\right)+3(V_{S1}^{(0)})^2R_\mu\kappa^2\right]\right.$$
$$\left.+\frac{676+2126\lambda+2176\lambda^2+1077\lambda^3}{14(1+\lambda)}\alpha^2\kappa^2\right\}\boldsymbol{e}_3+O(\kappa^3). \tag{38}$$

Consistent with our argument that the magnitude of the migration is given by that of the slip velocity times that of deformation, the leading-order contribution to the lift force is now $O(1)$ and is proportional to the product of the shear rate by the slip velocity. Hence in the limit $\kappa \to 0$ the direction of the migration is reversed if the direction of the shear or that of gravity is reversed. Moreover if $\alpha V_{S1}^{(0)}$ is negative (e.g. if the drop lags behind the fluid for a positive shear), (38) shows that an equilibrium position may exist near the wall provided $|V_{S1}^{(0)}/\alpha|$ is small enough. We are not aware of any detailed experiment in which the migration of a *buoyant* drop moving in a linear shear flow has been measured; hence we cannot validate (38) directly. Nevertheless we can return to the case of a neutrally buoyant drop for which we showed in § 3.4 that $V_{S1}^{(0)}$ reduces to $-\frac{\alpha}{8}R_S\kappa^2$. Then the contribution proportional to $(V_{S1}^{(0)})^2$ in (38) becomes of $O(\kappa^6)$ and those proportional to $\alpha V_{S1}^{(0)}$ and α^2 combine to give

$$\boldsymbol{F}_M^{(\delta)} = \frac{3\pi}{560}\frac{16+19\lambda}{(1+\lambda)^3}(27+51\lambda+27\lambda^2)\alpha^2R_\mu\kappa^2\boldsymbol{e}_3+O(\kappa^3). \tag{39}$$

Not surprisingly we recover the well-known κ^2-dependence of the migration of a neutrally buoyant drop in a linear shear flow, a result confirmed in several Couette flow experiments (Chan & Leal 1981; Smart & Leighton 1991), as well as in boundary element calculations (Uijttewaal *et al.* 1993; Uijttewaal & Nijhof 1995). The dependence on λ in (39) is identical to that obtained by Chaffey *et al.* (1965).

However, their numerical prefactor was exactly 11 times that found in (39). This was corrected by Chan & Leal (1979) who found a result identical to (39) (except for the intermediate coefficient, which they found to be 97/2 instead of 51 here and in Chaffey *et al.* 1965), and showed that experimental results (generally obtained with small λ) strongly support the magnitude of the force predicted by (39). This agreement with Chan & Leal (1979) allows us to validate most of the contributions in (38). Uijttewaal & Nijhof (1995) compared their numerical predictions with that of Chan & Leal (1979), i.e. with (39), over the whole range of λ. For λ less than unity, they found a good agreement with the theory for small values of the capillary number and large enough separations from the wall; this agreement deteriorates as the wall is approached, the theory overpredicting the migration by about 20% for $\kappa = 2/3$. In contrast, their results show that the present $O(\delta)$ theory behaves poorly for $\lambda > 1$ whatever κ, due to the fact that nonlinear $O(\delta^2)$ effects not accounted for tend to align the major axis of the drop with the direction of the flow (thus reducing the transverse migration), and the larger λ the larger this tendency.

6. The inertial migration and total force

6.1. *Fluid at rest at infinity*

As pointed out in the introduction, two different situations may in general be considered regarding the inertial migration. We first discuss the problem for the case where the fluid is at rest at infinity. When the distance κ^{-1} between the drop and the wall is much larger than the Oseen length scale G^{-1}, the wall lies in the Oseen region of the flow disturbance induced by the drop. Then, the situation is similar to that encountered in the unbounded case, with $O(G)$-inertia effects resulting in a singular perturbation problem. In contrast, when G/κ is much smaller than unity, the wall lies in the Stokes region of the flow disturbance. The image velocity field produced by the wall then combines with the primary flow disturbance in such a way that the resulting flow decays like r^{-2} in the far field. In this case, $O(G)$-inertia effects can be obtained through a regular perturbation process (Cox & Brenner 1968). This is the situation considered below. Hence our goal is to evaluate the inertial lift force due to wall effects under conditions $G \ll \kappa \ll 1$. Since we are looking for an approximation of the inertial lift force valid for large *and* moderate separations (typically $\kappa \leqslant 1/2$), we shall determine this force up to terms of $O(\kappa^2)$.

To evaluate the first volume integral in the right-hand side of (34*a*) we need to determine $\boldsymbol{U}^{(0)}$ and $\boldsymbol{u}$ everywhere in the external fluid up to terms of $O(\kappa^2)$. Up to now we have achieved this only in the inner region corresponding to $r \ll 1/\kappa$. Obtaining the uniformly valid expression $\bar{\boldsymbol{U}}^{(0)}$ (resp. $\bar{\boldsymbol{u}}$) of $\boldsymbol{U}^{(0)}$ (resp. $\boldsymbol{u}$) in outer variables $\bar{x}_i = \kappa x_i$ $(i = 1, 3)$, $\bar{r} = \kappa r$ is rather tedious because determining the image fields ${}_2\bar{\boldsymbol{U}}^{(0)}$ and ${}_2\bar{\boldsymbol{u}}$ everywhere requires an explicit evaluation of integral expressions of the type (A 2*b*). The corresponding technique is outlined in Appendix C. Using results (C 3)–(C 4) together with the inner expansions of $\boldsymbol{U}^{(0)}$ and $\boldsymbol{u}$ determined in § 3 and § 4, we are in position to evaluate the right-hand side of (34*a*). For this purpose, following Cox & Brenner (1968), we divide the flow domain into an inner region V_I and an outer region V_O such that

$$\left.\begin{aligned} V_I &= \{\boldsymbol{r} | 1 \leqslant r < \gamma_0 \kappa^{\chi-1}\}, \\ \bar{V}_O &= \{\bar{\boldsymbol{r}} | \gamma_0 \kappa^{\chi} < \bar{\boldsymbol{r}} < \infty,\ -1 \leqslant \bar{x}_3 < \infty\}, \end{aligned}\right\} \tag{40}$$

where γ_0 and χ are two arbitrary constants such that $\gamma_0 = O(\kappa^0)$ and $0 < \chi < 1$. Taking into account the transformations $\nabla \equiv \kappa\bar{\nabla}$ and $\mathrm{d}^3\boldsymbol{x} \equiv \kappa^{-3}\,\mathrm{d}^3\bar{\boldsymbol{x}}$, (34*a*) may now be written as

$$4\pi R_\mu \left(\sum_{n=0}^{2}(-1)^n J_D^n\right) V_{B3}^{(G)} = -\bar{\rho}\underbrace{\int_{V_B} \tilde{\boldsymbol{u}}\cdot(\tilde{\boldsymbol{U}}^{(0)}\cdot\nabla\tilde{\boldsymbol{U}}^{(0)})\,\mathrm{d}V}_{\mathscr{I}_B} - \underbrace{\int_{V_I}(\boldsymbol{u}+\boldsymbol{e}_3)\cdot(\boldsymbol{U}^{(0)}\cdot\nabla)\boldsymbol{U}^{(0)}\,\mathrm{d}^3\boldsymbol{x}}_{\mathscr{I}_I} - \kappa^{-2}\underbrace{\int_{\bar{V}_O}(\bar{\boldsymbol{u}}+\boldsymbol{e}_3)\cdot(\bar{\boldsymbol{U}}^{(0)}\cdot\bar{\nabla})\bar{\boldsymbol{U}}^{(0)}\,\mathrm{d}^3\bar{\boldsymbol{x}}}_{\mathscr{I}_O}. \tag{41}$$

Before we evaluate the right-hand side of (41), a careful examination of the various contributions is in order. First, since the inner domains V_I and V_B are symmetric with respect to all coordinates, it is easy to see that the leading-order contributions to $\mathscr{I}_I$ and $\mathscr{I}_B$ are of $O(\kappa^2)$. Hence only $\mathscr{I}_O$ contributes to the $O(1)$ and $O(\kappa)$ approximations of the inertial lift force. Second, we re-write the integrand of $\mathscr{I}_O$ truncated at $O(\kappa^4)$ in inner variables, multiply it by κ^{-2} and compare the result with the integrand of $\mathscr{I}_I$ truncated at $O(\kappa^2)$. This allows us to identify the part of integrand common to $\mathscr{I}_O$ and $\mathscr{I}_I$. Having done this, we may change the integration domain of $\mathscr{I}_O$ from $\bar{V}_O$ to $\bar{V}_O\cup\bar{V}_I$ (with $\bar{V}_I = \{\bar{\boldsymbol{r}}|\kappa \leqslant \bar{r} < \gamma_0\kappa^\chi\}$), provided we change the integral to be evaluated in V_I from $\mathscr{I}_I$ to $\mathscr{I}_I - \mathscr{I}_M$ where $\mathscr{I}_M$ is the contribution corresponding to the overlap. In fact, we may also change the domain of integration of $\mathscr{I}_I - \mathscr{I}_M$ from V_I to $V_I\cup V_O$ (with $V_O = \{\boldsymbol{r}|\gamma_0\kappa^{\chi-1} < r < \infty, -1 \leqslant x_3 < \infty\}$) because the integrand of $\mathscr{I}_I$ decays like r^{-5}, so that the corresponding contribution to V_O is of $O(\kappa^4)$, and hence negligible. Finally, we may simplify the evaluation of $\mathscr{I}_O$ by extending the integration domain of the outer contribution within the drop. There is no difficulty at $\bar{r} = 0$ because at the present order of approximation all the integrands in $\mathscr{I}_O$ are odd functions of $\bar{x}_3$, so that the singularity is integrable. Extending the domain of integration of the outer contribution within the drop changes the value $\mathscr{I}_O$ of the integral to another value $\mathscr{E}_O$, and we have to subtract explicitly the contribution $\mathscr{I}_T = -\kappa^{-2}(\mathscr{E}_O - \mathscr{I}_O)$ of the subdomain $\bar{V}_B = \{\bar{\boldsymbol{r}}|\bar{r} < \kappa\}$ from the right-hand side of (41). Taking into account all these remarks, it turns out that at the present level of approximation, (41) may be re-wrriten in the symbolic form

$$4\pi R_\mu \left(\sum_{n=0}^{2}(-1)^n J_D^n\right) V_{B3}^{(G)} = -\kappa^{-2}\mathscr{E}_O - \mathscr{I}_I + \mathscr{I}_M - \mathscr{I}_T - \bar{\rho}\mathscr{I}_B. \tag{42}$$

The next step is to decompose the various terms on the right-hand side of (42) into a collection of 'elementary' contributions, each of which is the product of an integral independent of both $\bar{\rho}$ and λ, and a single prefactor involving a combination of R_μ, D_μ, M_μ, and R_S. The result of this procedure, the expression for the corresponding integrals and their evaluation are detailed in a separate Appendix available upon request from the authors or the JFM Editorial Office. Using the results of this Appendix we finally obtain the inertial lift force acting on the drop as

$$\begin{aligned}\boldsymbol{F}_M^{(G)} &\approx 4\pi R_\mu\left(1 + \tfrac{3}{4}R_\mu\kappa + \tfrac{9}{16}R_\mu^2\kappa^2\right) V_{B3}^{(G)}\boldsymbol{e}_3 \\ &= \frac{\pi}{4}(V_{B1}^{(0)})^2 R_\mu^2\left\{1 + \frac{R_\mu}{8}\kappa + C_2(\lambda)\kappa^2\right\}\boldsymbol{e}_3 + O(\kappa^3),\end{aligned} \tag{43a}$$

with†

$$C_2(\lambda) \approx \frac{1320 + 2270\lambda + 1294\lambda^2 + 647\lambda^3}{1280(1+\lambda)^2(2+3\lambda)}. \tag{43b}$$

The leading-order contribution to the inertial lift force is positive and therefore directed away from the wall. As explained by McLaughlin (1993) and Hogg (1994), the physical mechanism that produces this force may be understood by considering the fluid displaced laterally by the drop as it translates. When this displaced fluid encounters the wall, the latter reacts by generating a lateral flow directed away from it, so that the associated pressure gradient is towards the wall. At large enough distances from the drop, this process becomes irreversible owing to inertia, and the lateral pressure gradient results in a lateral force directed away from the wall. As shown by (43*a*) the leading-order contribution to the force is proportional to the square of the strength R_μ of the Stokeslet in the unbounded solution (5*a*). Thus for instance, the leading-order inertial lift force on an inviscid bubble is $(2/3)^2 \approx 0.444$ that on a solid sphere. As will become apparent in the next sections, this is a general feature of leading-order inertial effects, and this feature is not restricted to near-wall situations, neither does it depend on the regular or singular nature of the problem, as was shown by Legendre & Magnaudet (1997). The $O(1)$ term in (43*a*) was obtained by Vasseur & Cox (1976) and Cox & Hsu (1997) for the particular case of a rigid sphere. It must be kept in mind that this leading-order expression yields the value of the lift force in the limit $\kappa \to 0$ under the condition $G/\kappa \ll 1$ corresponding to the case where the wall is close to the *outer* limit of the Stokes region of the flow disturbance. The complementary case where the wall lies in the Oseen region ($G/\kappa \gg 1$) of the flow disturbance was considered by Vasseur & Cox (1977) for a rigid sphere and by Takemura *et al.* (2002) for an inviscid spherical bubble. In this situation Vasseur & Cox found that the lift force, $\boldsymbol{F}_{MO}$ say, is a function of G/κ, which for small values of G/κ takes the value $\boldsymbol{F}_{MO}(G/\kappa \to 0, \lambda \to \infty) = (9\pi/16)G(V_{B1}^{(0)})^2\boldsymbol{e}_3$ (with the present normalization), while Takemura *et al.* obtained $\boldsymbol{F}_{MO}(G/\kappa \to 0, \lambda = 0) = (\pi/4)G(V_{B1}^{(0)})^2\boldsymbol{e}_3$ (see their equation (A 9)). These values are identical to the leading-order term of (43*a*) as they should be, since small values of G/κ in $\boldsymbol{F}_{MO}$ correspond to the case where the wall lies near the *inner* limit of the Oseen region, and the solution given by (43) must then match with $\boldsymbol{F}_{MO}$.

A striking feature in (43*a*) is that the $O(G)$-inertial lift force does not depend on the drop density. This is unexpected at first glance, since (41) suggests that inertial terms associated with the motion inside the drop should in principle contribute to the lift force at $O(\kappa)^2$. However, it turns out that the corresponding integrals vanish for subtle symmetry reasons. We note that in their investigation of the small inertial effects experienced by a drop moving in an unbounded fluid, Taylor & Acrivos (1964) found that the drag force is affected by the drop density only at $O(We)$. Since the Weber number is $We = G\delta$ in the present notation, their result suggests that in the present problem the lift force probably depends on $\bar{\rho}$ only through higher-order terms (with respect to G and δ) not accounted for in the present approximation.

† Some of the integrals required to obtain the coefficient C_2 of (43*a*) and the coefficient D_1 of (45*a*) were evaluated numerically with a precision of three digits. Hence, the values of these coefficients must be considered as approximations; this is why we use the symbol $\approx$ in (43*b*) and (45*b*).

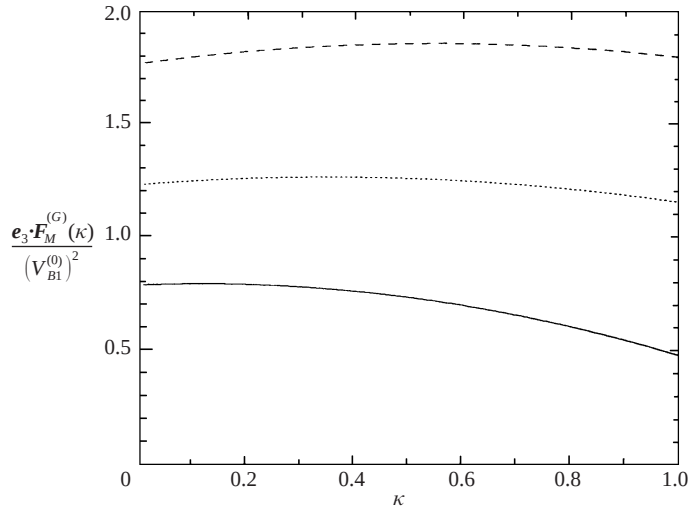

FIGURE 7. The normalized inertial lift force as a function of the distance to the wall, as predicted by (44) (fluid at rest at infinity): ——, $\lambda = 0$; · · · · · ·, $\lambda = 1$; – – –, $\lambda \to \infty$.

For an inviscid bubble, (43) yields†

$$\boldsymbol{F}_M^{(G)}/(V_{B1}^{(0)})^2 \approx \frac{\pi}{4}\{1 + 0.125\kappa - 0.516\kappa^2\}\boldsymbol{e}_3 + O(\kappa^3), \tag{44a}$$

whereas for a solid sphere or a very viscous drop

$$\boldsymbol{F}_M^{(G)}/(V_{B1}^{(0)})^2 \approx \frac{9\pi}{16}\{1 + 0.1875\kappa - 0.168\kappa^2\}\boldsymbol{e}_3 + O(\kappa^3). \tag{44b}$$

These results are plotted in figure 7 together with that corresponding to homoviscous fluids. The $O(\kappa)$-term produces a slight increase of the normalized force (which may be interpreted as a lift coefficient) as the distance between the drop and the wall decreases. However, this effect is rapidly overwhelmed by that of the negative $O(\kappa^2)$-term. In the case of a rigid sphere both terms are small and of similar magnitude, so that the normalized force experiences little variation as κ increases. Equation (44*b*) compares well with the numerical results of Fisher & Rosenberger (1987) obtained for $\kappa \leqslant 0.8$ and with the fit determined by Cherukat & McLaughlin (1994) after a numerical evaluation of the volume integral on the right-hand side of (34*a*) for $0.05 \leqslant \kappa \leqslant 0.9$, the integrand having been obtained by using an exact solution of Stokes equation valid whatever the separation distance between the sphere and the wall. In the limit case where the sphere touches the wall ($\kappa = 1$), (44*b*) predicts $\boldsymbol{F}_M^{(G)}/(V_{B1}^{(0)})^2 \approx 1.802$, a value only 2.5% higher than the exact value 1.755 determined by Krishnan & Leighton (1995); although unexpected, this agreement is noticeable. Using the lateral force balance (34*a*) and the approximate expression for the lateral drag force (30*b*) (or better the higher-order approximation (51*b*) derived below), the normalized migration velocity $V_{B3}^{(G)}/(V_{B1}^{(0)})^2$ predicted by (44*b*) may also be compared with the results of Becker *et al.* (1996) who employed a technique similar to that of Cherukat & McLaughlin (1994). Both series of results are in excellent agreement for $\kappa \leqslant 0.7$ and show that the large increase of the lateral drag coefficient near the wall makes $V_{B3}^{(G)}/(V_{B1}^{(0)})^2$ decrease

† We also evaluated the $O(\kappa^3)$ term for an inviscid bubble and found that the corresponding coefficient is −0.034.

continuously from the value 3/32 corresponding to the limit $\kappa \to 0$ (Cox & Hsu 1977), to values about 0.025 for $\kappa = 0.7$. For smaller separations, neither (30*b*) nor (51*b*) predicts accurately the lateral drag (see § 7), and the agreement rapidly deteriorates.

In contrast to the behaviour observed for a rigid sphere, the lift force experienced by an inviscid bubble decreases significantly as the distance to the wall decreases. As shown in figure 7, (44*a*) predicts that the limit value for to $\kappa = 1$ is only about 60% of that corresponding to $\kappa \to 0$. This difference comes from the 'inner' contribution to the lift force provided by the region $r \ll 1/\kappa$. This contribution is zero for an inviscid bubble whereas, owing to the presence of dipoles and quadrupoles in the solution (5*a*)–(8*a*), it provides a positive contribution about 0.7 to the coefficient C_2 for a rigid sphere.

Most experimental data available for a rigid sphere (Vasseur & Cox 1977; Cherukat & McLaughlin 1990) concern the case where the wall lies in the Oseen region of the flow disturbance. Some of these data were however obtained in the situation $G \ll \kappa \ll 1$ considered here. These data essentially confirm the magnitude of the leading-order term of (44*b*). However, owing to the significant experimental uncertainty affecting the determination of the migration velocity, the evolution of the lateral force as κ increases does not show a clear tendency, thus preventing a convincing check on the accuracy of higher-order contributions in (44*b*). Similarly, the leading-order term of (44*a*) was recently confirmed by Takemura *et al.* (2002), who performed experiments with spherical bubbles rising near a vertical wall in silicone oil. Again, a convincing comparison of experimental data with higher-order terms in (44*a*) is not possible, partly because of the increase in the experimental uncertainty as the wall is approached, but also because the deformation-induced lift force determined in § 5 becomes significant or even dominant as κ increases.

6.2. *Linear shear flow*

Let us now consider the case of a buoyant drop moving in a linear shear flow. Then the wall lies in the Stokes region of the flow disturbance provided κ^{-1} is much smaller than both the Oseen length scale G^{-1} and the Saffman length scale $(\alpha G)^{-1/2}$. If these conditions are satisfied and inertial effect remain small, i.e. $\alpha G \ll \kappa^2 \ll 1$ and $G \ll \kappa \ll 1$, Cox & Hsu (1977) established that the method initially developed by Cox & Brenner (1968) for a stagnant fluid or a shear flow bounded by two walls applies without modification to the case of linear and parabolic flows bounded by a single wall. Hence the $O(G)$-inertial lift force may be obtained by applying the techniques described in § 6.1 to the velocity fields $\boldsymbol{U}^{(0)}$ and $\tilde{\boldsymbol{U}}^{(0)}$ defined by (5), (7), (8), (10) and (21). To avoid too cumbersome calculations we have determined only the $O(\kappa)$-approximation of the lift force in this type of flow. The corresponding velocity field $\bar{\boldsymbol{U}}^{(0)}$ is given by (C 5). We note that in (41) the contributions of $\mathscr{I}_I$ and $\mathscr{I}_B$ are now a *a priori* of $O(\kappa^0)$ because the shear produces even integrands at this order. The corresponding contributions, independent of the presence of the wall, provide the so-called second-order Saffman lift force whose magnitude is $\frac{7}{8}\pi\alpha V_{S1}^{(0)}$ for a freely rotating rigid sphere translating with a slip velocity $V_{S1}^{(0)}$ (Saffman 1965). Evaluating the various contributions to (42) along the lines described in § 6.1 yields

$$\begin{aligned}\boldsymbol{F}_M^{(G)} &\approx 4\pi R_\mu \left(1 + \tfrac{3}{4} R_\mu \kappa\right) V_{B3}^{(G)} \boldsymbol{e}_3 \\ &= \left[\tfrac{11}{24}\pi \left(-\alpha V_{S1}^{(0)} R_\mu^2 \{\kappa^{-1} + D_0(\lambda) + D_1(\lambda)\kappa\} + \tfrac{1}{3}\alpha^2 R_\mu R_S \left\{1 + \tfrac{3}{8} R_\mu \kappa\right\}\right)\right. \\ &\quad \left. + \frac{\pi}{4}(V_{S1}^{(0)})^2 R_\mu^2 \left\{1 + \frac{R_\mu}{8}\kappa\right\}\right] \boldsymbol{e}_3 + O(\kappa^2), \end{aligned} \tag{45a}$$

with

$$D_0(\lambda) = \frac{3960 + 12444\lambda + 14826\lambda^2 + 6645\lambda^3}{880(2+3\lambda)^2(1+\lambda)}, \quad D_1(\lambda) = \frac{3(75 + 222\lambda + 257\lambda^2 + 104\lambda^3)}{110(2+3\lambda)(1+\lambda)^2}. \tag{45b}$$

The lift force, which again does not involve the drop density at the present order of approximation, now possesses two shear-induced contributions. The first of them is due to the interaction of the shear with the slip velocity and changes sign when α or $V_{S1}^{(0)}$ is reversed. The second contribution is always positive, i.e. directed away from the wall, and arises from the interaction of the stresslet of (21*a*) with the wall. If $\alpha V_{S1}^{(0)}$ is positive (e.g. if the drop leads the fluid for a positive shear rate), the first term in the right-hand side pushes the drop towards the wall and an equilibrium position may exist for high enough shear rates. The leading-order term (with respect to κ) is still proportional to R_μ^2, i.e. to the square of the intensity of the stokeslet in (5*a*), but this term is now of $O(\kappa^{-1})$. This means that the corresponding force increases as the distance between the drop and the wall increases. However, it must be kept in mind that κ must remain large compared with $(\alpha G)^{1/2}$ for the result (45*a*) to be valid. When κ becomes comparable to $(\alpha G)^{1/2}$, i.e. the distance to the wall becomes of the order of the Saffman length, the corresponding lift force $G\boldsymbol{F}_M^{(G)}$ becomes of $O((\alpha G)^{1/2})$. This is precisely the order of magnitude of the Saffman lift force experienced by a particle moving in an unbounded linear shear flow (Saffman 1965). Thus one may say that the wall inhibits the Saffman lift force, since (45*a*) indicates that the magnitude of the force changes from $O((\alpha G)^{1/2})$ for $\kappa = O((\alpha G)^{1/2})$ to $O(\alpha G)$ for $\kappa = O(1)$. A physical interpretation of this force, which does not require the presence of the wall, was given by Hogg (1994). If the drop leads the flow, the velocity difference between the fluid it displaces laterally and the undisturbed flow is smaller in the direction of increasing velocity, thus inducing a lateral pressure gradient in the same direction. At large enough distances from the drop, the displacement process becomes irreversible and the lateral pressure gradient results in a lateral force in the direction of decreasing velocity. The reverse argument shows that the migration reverses if the drop lags behind the fluid.

The α^2-term is proportional to the product of the strength of the stokeslet in (5*a*) and that of the stresslet in (21*a*). This term provides the leading contribution in the situation where the drop is neutrally buoyant. In this case, combining (23*b*) and (45*a*), we obtain the $O(\kappa)$-approximation

$$\boldsymbol{F}_M^{(G)} = \tfrac{11}{72}\pi\alpha^2 R_\mu R_S \left(1 + \tfrac{3}{4}R_\mu\kappa\right)\boldsymbol{e}_3 + O(\kappa^2). \tag{46}$$

The leading-order term agrees with the value found by Cox & Hsu (1977) for a rigid sphere. This situation was considered numerically by Fisher & Rosenberger (1987), still for a rigid sphere. Comparing (46) with their numerical curve reveals a good agreement for $\kappa < 0.3$, whereas for smaller separations the higher-order contributions not accounted for in (46) make the force increase significantly. Coming back to the general situation of a buoyant drop, we see that in the case of an inviscid bubble, (45*a*) becomes

$$\boldsymbol{F}_M^{(G)} = \frac{\pi}{4}\Big[-\tfrac{11}{6}\alpha V_{S1}^{(0)}(\kappa^{-1} + 1.125 + 1.023\kappa) + \tfrac{11}{18}\alpha^2(1 + 0.375\kappa) + (V_{S1}^{(0)})^2(1 + 0.125\kappa)\Big]\boldsymbol{e}_3 + O(\kappa^2), \tag{47a}$$

whereas for a very viscous drop or a rigid sphere we have

$$\boldsymbol{F}_M^{(G)} = \tfrac{9}{16}\pi\Big[-\tfrac{11}{6}\alpha V_{S1}^{(0)}(\kappa^{-1} + 0.839 + 0.945\kappa) + \tfrac{55}{54}\alpha^2(1 + 0.5625\kappa) + (V_{S1}^{(0)})^2(1 + 0.1875\kappa)\Big]\boldsymbol{e}_3 + O(\kappa^2). \tag{47b}$$

In both cases the higher-order (i.e. $O(\kappa^0)$ or $O(\kappa)$) contributions increase the magnitude of the lift force as the separation distance to the wall decreases, a conclusion in agreement with the fit determined by Cherukat & McLaughlin (1994) for a rigid sphere. Moreover the $O(\kappa^0)$-truncation of (47b) agrees exactly with that obtained by Lovalenti in an Appendix to the aforementioned paper, suggesting that (45) is correct at least at up to $O(\kappa^0)$ (the fit of Cherukat & McLaughlin 1994 indicates 0.254 instead of 0.945 for the $O(\kappa)$ term in the first parentheses). For practical purposes, it is interesting to notice that in the limit case of a freely rotating rigid sphere in contact with a wall, the $O(\kappa^0)$ truncation of (47b) gives an accurate estimate of the force. More precisely, if the relative velocity $V_{S1}^{(0)}$ is zero (resp. $-\alpha$, corresponding to a sphere prevented from translating with respect to the wall), the $O(\kappa^0)$ truncation of (47b) predicts a dimensionless force of 1.80 (resp. 9.525) which agrees within 5% with the exact value 1.6915 (resp. 10.0) determined by Krishnan & Leighton (1995). This surprising agreement is due to the fact that higher-order contributions to the force almost cancel mutually in the limit $\kappa \to 1$.

6.3. *The total force*

Since we have determined both the inertial and deformation-induced contributions to the lift force and have assumed that the Ohnesorge number $Oh = G/\delta$ is of $O(1)$, we can finally write an expression for the total lift force (normalized by $\rho|1-\bar{\rho}|R^3 g$). For the case of a fluid at rest at infinity, (36) and (43a) may be combined in the form

$$\boldsymbol{F}_M \approx \frac{\pi}{4} G(V_{B1}^{(0)})^2 R_\mu^2 \left\{ 1 + \frac{R_\mu}{8}\kappa + C_2(\lambda)\kappa^2 + \tfrac{3}{40}\frac{16+19\lambda}{(2+3\lambda)}\frac{(2-10\lambda+3\lambda^2)}{(1+\lambda)^2} Oh^{-1}\kappa^2 \right\} \boldsymbol{e}_3, \tag{48}$$

with $C_2(\lambda)$ given by (43b). It is worth noting that since the rotation of the fluid inside the drop affects the solution only at $O(\kappa^4)$, (48) also applies to the case of a non-rotating rigid particle fixed in a uniform flow of velocity $-V_{B1}^{(0)}$, the particle Reynolds number being then $Re = -GV_{B1}^{(0)}$. Similarly, (45a) can be combined with (38) to obtain the $O(\kappa)$-approximation of the total lift force experienced by a buoyant drop moving in a linear shear flow. Defining the relative shear rate $S = \alpha/V_{S1}^{(0)}$, the result takes the form

$$\boldsymbol{F}_M \approx \frac{\pi}{4} G(V_{S1}^{(0)})^2 R_\mu^2 \left[1 + \frac{R_\mu}{8}\kappa - \tfrac{11}{6} S \left\{ (\kappa^{-1} + D_0(\lambda) + D_1(\lambda)\kappa) - \tfrac{12}{55} Oh^{-1} \frac{16+19\lambda}{(1+\lambda)} \frac{(2-10\lambda+3\lambda^2)}{(2+3\lambda)^2} \left(1 + \tfrac{3}{8}R_\mu\kappa\right) \right\} + \tfrac{11}{18}\frac{R_S}{R_\mu} S^2 \left(1 + \tfrac{3}{8}R_\mu\kappa\right) \right] \boldsymbol{e}_3 + O(\kappa^2), \tag{49}$$

with $D_0(\lambda)$ and $D_1(\lambda)$ given by (45b). Note that for most values of λ, the inertial and deformation-induced contributions to the S-term have opposite signs, so that for $O(1)$-Ohnesorge numbers the deformation generally reduces or even reverses the total lift force. We may observe that for $\kappa \to 1$, the prefactor of the Ohnesorge

number in (48)–(49) and the inertial term are both of $O(1)$. Hence it turns out that for $O(1)$-Ohnesorge numbers, inertial effects cannot be neglected in the prediction of the migration velocity, however small the Reynolds number and the distance to the wall. In practice, situations where the migration of bubbles or slightly viscous drops can be predicted by considering only the contribution of the deformation are indeed restricted to highly viscous liquids. For instance, consider a bubble with $R = 1\,\mathrm{mm}$ rising in a stagnant bath of oil with a reduced surface tension $\gamma/\rho = 2 \times 10^{-5}\,\mathrm{m^3\,s^{-2}}$. Then, according to (48), the deformation-induced migration is one order of magnitude larger than the inertial migration only if the viscosity of the suspending fluid is larger than 0.3 P.

It is finally interesting to examine the $O(\delta)$ and $O(G)$ corrections to the drag force, which may be readily obtained by considering the appropriate form of the reciprocal theorem. Using (4*c*), it is straightforward to show that this form is identical to (34*a*, *b*) with quantities associated with the complementary problem considered in § 4 replaced by their counterparts corresponding to the 'direct' problem solved in § 3. Expressing the various integrals then reveals that the surface (resp. volume) integrals involved in the $O(\delta)$ (resp. $O(G)$) problem have integrands that are odd functions of x_3 (resp. x_1). Consequently, all contributions integrate to zero, yielding

$$V_{B1}^{(\delta)} = V_{B1}^{(G)} = 0. \tag{50}$$

Thus deformation does not affect the drag at the present order of approximation. Moreover, unlike to what happens in an unbounded flow or when the wall lies in the Oseen region of the flow disturbance (e.g. Vasseur & Cox 1977), there is no inertial correction to the drag force at $O(G)$. This is because (34*a*) only involves the Stokes solution (as opposed to the Oseen solution) of the problem, and it may be shown from symmetry considerations that the inertial contribution based on the former solution may only lead to a transverse contribution to the force (Lovalenti & Brady 1993).

7. A buoyant drop in a linear shear flow near a horizontal wall

In this section we briefly consider the case of a buoyant drop moving in a linear shear flow near a *horizontal* wall. Let $V_{B3}^{(0)}$ be the $O(1)$ vertical velocity of the drop, corresponding to the creeping flow problem around a spherical drop. Then at order zero in δ and G the drag force at $O(\kappa^3)$ is just $V_{B3}^{(0)}$ times the force $\boldsymbol{F}_{DC}$ given by (29). In addition there is an $O(\kappa^2)$-slip velocity $V_{S1}^{(0)}$ given by (23*b*) between the drop and the local flow. Owing to the linearity of the Stokes equation, the deformation of the drop is $V_{B3}^{(0)}$ times the deformation $f_\perp$ given by (31) plus the contribution proportional to the shear rate α in (24). The previous estimates of $\boldsymbol{F}_{DC}$ and $f_\perp$ can be slightly improved near the wall by using the procedure described in § 3.3. Details of the calculations are provided in Appendices A and B. For instance, the correction factor K_{SDC} given by (B6) can be used to determine the $O(\kappa^5)$-approximation of the drag force near the wall. We obtain for an inviscid bubble

$$\boldsymbol{F}_{DC} \approx -4\pi V_{B3}^{(0)} \left[1 - \tfrac{3}{4}\kappa - \tfrac{9}{64}\kappa^4\right]^{-1} \boldsymbol{e}_3, \tag{51a}$$

whereas for a very viscous drop or a solid sphere we have

$$\boldsymbol{F}_{DC} \approx -6\pi V_{B3}^{(0)} \left[1 - \tfrac{9}{8}\kappa + \tfrac{1}{2}\kappa^3 - \tfrac{135}{256}\kappa^4 - \tfrac{1}{8}\kappa^5\right]^{-1} \boldsymbol{e}_3. \tag{51b}$$

These results agree with those of Fuentes, Kim & Jeffrey (1988). Since (51*b*) predicts that the drag force on a rigid sphere becomes infinite for $\kappa \approx 0.85$ whereas it is well

known that the exact solution yields an infinite drag only for $\kappa = 1$ (Brenner 1961; Happel & Brenner 1973, pp. 330–331), we have to conclude that the approximation underlying (51a, b) breaks down close to the wall. This is not unexpected since the reflection technique starts from the unbounded solution in which the streamlines exhibit a fore–aft symmetry and is used here to approximate a flow where the streamlines experience a very severe distortion near the stagnation point located at the intersection of the wall and the symmetry axis of the flow. In § 6 we pointed out that our prediction for the inertial migration velocity of a rigid sphere (in which the expression (51b) for $\boldsymbol{F}_{DC}$ was used) compares very well with the numerical solution of Becker *et al.* (1996) up to $\kappa \approx 0.7$. In contrast, the predicted values were found to become too small for smaller separations. Since the normalized migration force (44b) still agrees well with the numerical predictions of Cherukat & McLaughlin (1994) for $\kappa > 0.7$, we infer that the underprediction of the migration velocity in this range of κ is due to an overestimate of the drag force in (51b). Consequently we guess that the limit of validity of (51) near the wall is about $\kappa = 0.7$.

Let us now consider the corrections to the drag force and slip velocity due to deformation. Given the deformation predicted by (31) and the α^2-term in the force predicted by (38), the vertical drag force experiences corrections $O(\delta(V_{B3}^{(0)})^2\kappa^2)$ and $O(\delta\alpha^2\kappa^2)$, the latter being directly given by (39). To evaluate the former contribution, we use (35) with all quantities associated with a translation along the x_1-axis replaced by their counterpart for a translation along the x_3-axis. The complete result is then

$$\boldsymbol{F}_M^{(\delta)} \cdot \boldsymbol{e}_3 = \frac{3\pi}{160}\frac{16+19\lambda}{(1+\lambda)^3} R_\mu \kappa^2 \left[(2-10\lambda+3\lambda^2)(V_{B3}^{(0)})^2 + \tfrac{2}{7}(27+51\lambda+27\lambda^2)\alpha^2\right] + O(\kappa^3). \tag{52}$$

Note that the λ-dependence of the first term within square brackets is the same as that found in (36). Both contributions are positive for most values of λ, i.e. they generally increase the drag when the drop moves towards the wall whereas they provide a thrust force when it recedes from the wall. It is easy to see that the deformation proportional to $\alpha x_1 x_3/r^2$ in (24) results in a $O(\delta)$-force in the horizontal direction. To evaluate this contribution, we just need to note that in the form (35) of the reciprocal theorem, the roles of $\boldsymbol{U}^{(0)}$ and $\boldsymbol{u}$, i.e. those of x_1 and x_3, $\boldsymbol{e}_1$ and $\boldsymbol{e}_3$, should be interchanged compared to the situation considered in § 5. Consequently the intensity of the force is identical to that given by the first term in the right-hand side of (38), i.e. we have

$$\boldsymbol{F}_M^{(\delta)} \cdot \boldsymbol{e}_1 = \frac{\pi}{40}\frac{16+19\lambda}{(1+\lambda)^3}(2-10\lambda+3\lambda^2)\alpha V_{B3}^{(0)}\left(1+\tfrac{3}{8}R_\mu\kappa\right) + O(\alpha\kappa^2). \tag{53}$$

To evaluate inertial corrections we must first estimate the influence of unsteadiness in the present problem. Unsteadiness exists in the vertical direction because the drop accelerates or decelerates as its distance to the wall varies, so as to maintain a constant drag. The horizontal velocity of the drop also varies in time because the drop crosses the streamlines of the shear flow and must maintain a weak slip in order to satisfy the zero-force condition. Consequently the reference frame attached to the drop centroid is not strictly inertial and a complementary acceleration must be introduced. Since the characteristic time scale is $\mu/(\rho|1-\bar{\rho}|gR)$ (we exclude the initial acceleration stage), the right-hand side of the momentum equations (2a) now includes terms $G\delta(\boldsymbol{U}+\boldsymbol{V}_B)/\partial t$ in the suspending fluid and $(\bar{\rho}G/\lambda)\delta(\tilde{\boldsymbol{U}}+\boldsymbol{V}_B/\partial t)$ within the drop, t denoting the dimensionless time. To estimate the magnitude of these terms along the $\boldsymbol{e}_3$-direction, we use the fact that $V_{B3}^{(0)}\boldsymbol{F}_{DC}$ is independent of time. From this and (29) we deduce that $\partial V_{B3}^{(0)}/\partial t$ is $O(V_{B3}^{(0)}\partial\kappa/\partial t)$. Noting that the vertical velocity of

the drop centroid is the time-derivative of the separation distance $1/\kappa$, we conclude that $\partial V_{B3}^{(0)}/\partial t = O((V_{B3}^{(0)})^2\kappa^2)$. In the horizontal direciton, we know from (23*b*) that $V_{B1}^{(0)} = \alpha/\kappa + O(\alpha\kappa^2)$, so that we may write

$$\frac{\partial V_{B1}^{(0)}}{\partial t} = \frac{\partial V_{B1}^{(0)}}{\partial(1/\kappa)}\frac{\mathrm{d}(1/\kappa)}{\mathrm{d}t} = \alpha V_{B3}^{(0)}(1 + O(\kappa^3)).$$

In the reference frame attached to the drop, the undisturbed flow has a non-zero acceleration $-\alpha V_{B3}^{(0)}\boldsymbol{e}_1$ and the leading-order contribution provided by the complementary acceleration $\mathrm{d}\boldsymbol{V}_B/\mathrm{d}t$ just cancels it. Consequently the actual unsteadiness in the horizontal direction is of $O(\kappa^3\alpha V_{B3}^{(0)})$. By extending the reciprocal theorem to include the unsteady terms, it can be shown that at leading order the integrals associated with these contributions involve the product of two stokeslets, so that they are multiplied by κ^{-1} when expressed in outer variables. Hence, using the above estimates, we conclude that the leading-order contribution of unsteadiness in the total force is $O(G(V_{B3}^{(0)})^2\kappa)$ in the vertical direction and $O(G\alpha V_{B3}^{(0)}\kappa^2)$ in the horizontal one. Therefrom we may evaluate vertical (resp. horizontal) inertial corrections up to $O(G(V_{B3}^{(0)})^2)$ (resp. $O(G\alpha V_{B3}^{(0)}\kappa)$) without considering unsteady effects, except those due to the complementary acceleration.

By inspection we see that the vertical drag force may have corrections of $O(G(V_{B3}^{(0)})^2)$ and $O(G\alpha^2)$, the latter being given by (46). However, changing $\boldsymbol{U}^{(0)}$ to $V_{B3}^{(0)}\boldsymbol{u}$ in (34*a*) reveals that the $O(1)$ inertial term related to the rise/fall velocity is zero. Hence we simply obtain at leading order

$$\boldsymbol{F}_M^{(G)} \cdot \boldsymbol{e}_3 = \tfrac{11}{72}\pi R_\mu R_S \alpha^2 + O(\kappa\alpha^2, \kappa(V_{B3}^{(0)})^2). \tag{54}$$

Again this term increases (resp. decreases) the drag when the drop moves towards (resp. away from) the wall. This conclusion agrees with that of Hogg (1994) who studied the sedimentation of a rigid particle in a horizontal Poiseuille flow in the case where the wall lies in the Oseen region of the disturbance. Equations (52), (54) and (29) (or (51)) may now be combined to find how the wall modifies the rise/settling velocity of the drop. For instance, in the case of a negatively buoyant rigid sphere ($\bar{\rho} > 1$) falling towards the wall, (51*b*), (54) and (3*b*) (with $\boldsymbol{e}_1$ replaced by $\boldsymbol{e}_3$) yield the sedimentation velocity

$$V_{B3} = V_{B3}^{(0)} + GV_{B3}^{(G)} = -\tfrac{2}{9}\left[1 - \tfrac{9}{8}\kappa + \tfrac{1}{2}\kappa^3 - \tfrac{135}{256}\kappa^4 - \tfrac{1}{8}\kappa^5\right]\left(1 - \tfrac{55}{128}G\alpha^2\right). \tag{55}$$

For $\kappa = 0.5$, the influence of the first term reduces the sedimentation velocity to 46% of its free-stream value, and this reduction is further enhanced by the inertial correction.

Now changing $\boldsymbol{u} + \boldsymbol{e}_3$ to $\boldsymbol{U}^{(0)}/V_{B1}^{(0)} + \boldsymbol{e}_1$ and $\boldsymbol{U}^{(0)}$ to $V_{B1}^{(0)}\boldsymbol{u} + \boldsymbol{U}_\alpha^{(0)}$ in (34*a*) (with $\boldsymbol{U}^{(0)}$, $\boldsymbol{U}_\alpha^{(0)}$, and $\boldsymbol{u}$ as determined in § 3.1, § 3.4 and § 4, respectively), we may evaluate the horizontal force produced by the interaction of the shear with the vertical velocity. Truncating at $O(\kappa^0)$ we then obtain

$$\boldsymbol{F}_M^{(G)} \cdot \boldsymbol{e}_1 = -\tfrac{5}{8}\pi R_\mu^2(\kappa^{-1} - E_0(\lambda))\alpha V_{B3}^{(0)} + O(\kappa\alpha V_{B3}^{(0)}), \tag{56a}$$

with

$$E_0(\lambda) = \frac{4840 + 14100\lambda + 11934\lambda^2 + 2191\lambda^3}{1200(2 + 3\lambda)^2(1 + \lambda)}. \tag{56b}$$

Note that while this is not directly apparent, the $O(\kappa^0)$ term comprises contributions due to the horizontal acceleration of the fluid entrained by the drop (i.e. added-mass effects). It must also be stressed that (56) only apply to the present situation

where the horizontal slip is small; if the drop were prevented from moving along the horizontal direction, the above results would be changed by positive contributions due to unsteadiness. The leading-order term in (56*a*) is a lift force parallel to the wall that tends to maintain the drop behind the flow if $\alpha V_{S3}^{(0)}$ is positive. This effect also exists in an unbounded flow. The corresponding force is $O((\alpha G)^{1/2})$ and was first evaluated in the low-Reynolds-number limit by Harper & Chang (1968), and later reconsidered by Hogg (1994). A reasoning similar to that of § 6.2 shows that the leading-order term of (56*a*) is simply what is left of this effect in the vicinity of the wall. It is worth noting that the physical interpretation of this effect is somewhat different from the explanation given for the leading-order shear-induced lift force in (45) because the drop now crosses the streamlines of the shear flow. Suppose that the drop moves in the direction of increasing velocity of the shear flow. Then the fluid contained in the wake experiences a transverse velocity that decreases as the downstream distance increases, and this results in a bending of the wake. Owing to continuity, this curved wake generates a counterflow with negative transverse velocities. At sufficiently large distances from the drop this process becomes irreversible and the pressure gradient sets up by the counterflow induces a negative transverse force on the drop, making it lag behind the undisturbed flow (the reverse argument applies for a drop moving in the direction of decreasing velocity, and the corresponding migration makes the drop leading the flow).

To obtain the improved approximation of the horizontal slip velocity $V_{S1} = V_{S1}^{(0)} + GV_{S1}^{(G)} + \delta V_{S1}^{(\delta)}$, we use the zero-force condition along the $\boldsymbol{e}_1$-axis. The force balance is written

$$\tfrac{4}{3}\pi G\bar{\rho}\frac{\mathrm{d}\boldsymbol{V}_B}{\mathrm{d}t}\cdot\boldsymbol{e}_1 = (\boldsymbol{F}_D + G\boldsymbol{F}_M^{(G)} + \delta\boldsymbol{F}_M^{(\delta)})\cdot\boldsymbol{e}_1,$$

with the deformation-induced force and the inertial force given by (53) and (56) respectively, the drag force being given by (23*a*) with $V_{S1}^{(0)}$ replaced by V_{S1}. This yields

$$V_{S1} = -\frac{\alpha}{8}R_S\kappa^2 + G\left\{\frac{Oh^{-1}}{80}\frac{16+19\lambda}{2+3\lambda}\frac{(2-10\lambda+3\lambda^2)}{(1+\lambda)^2}\right.$$
$$\left. -\frac{\bar{\rho}}{3R_\mu} - \tfrac{5}{32}R_\mu\left(\kappa^{-1} - \tfrac{3}{8}R_\mu - E_0(\lambda)\right)\right\}\alpha V_{B3}^{(0)} + O(\alpha\kappa^4, \alpha\delta\kappa^2, \alpha G\kappa), \qquad (57)$$

with $E_0(\lambda)$ given by (56*b*). Very close to the wall, the first term in the right-hand side is clearly dominant. In contrast, as κ decreases, terms due to deformation or inertia may become larger (note however that the inertial term remains small compared to κ, owing to the condition $\alpha G \ll \kappa^2$). Given the positive sign of the deformation-induced term for most λ, the drop generally leads the fluid if deformation effects are dominant whereas it lags behind it otherwise.

8. Summary

We have derived analytical expressions for the drag and lift forces acting on a buoyant drop of arbitrary viscosity moving in a viscous fluid at rest or in a linear shear flow near a wall. These results show how the wall increases the drag force and modifies the deformation experienced by the drop in an unbounded flow. We also evaluated effects of finite inertia and deformation in the limit of small Galileo and Bond numbers (with the restriction that inertial corrections are valid only in the vicinity of the wall, owing to conditions $G \ll \kappa$ and $\alpha G \ll \kappa^2$). On the basis of comparisons with available numerical solutions or experiments, we showed that most

	Inviscid bubble	Very viscous drop/rigid sphere
(*a*) Drag (equation (16))	$\boldsymbol{F}_D \approx -4\pi V_{B1}^{(0)}\left[1-\frac{3}{8}\kappa-\frac{3}{64}\kappa^4\right]^{-1}\boldsymbol{e}_1$	$\boldsymbol{F}_D \approx -6\pi V_{B1}^{(0)}\left[1-\frac{9}{16}\kappa+\frac{1}{8}\kappa^3-\frac{45}{256}\kappa^4-\frac{1}{16}\kappa^5\right]^{-1}\boldsymbol{e}_1$ (Faxén 1921)
Deformation (equation (19))	$f_2^{(\delta)} \approx \frac{3}{4}V_{B1}^{(0)}\kappa^2\left[1+\frac{3}{8}\kappa\left(1+\frac{3}{8}\kappa+\frac{73}{64}\kappa^2\right)\right]\frac{x_1x_3}{r^2}$	$f_2^{(\delta)} \approx \frac{171}{128}V_{B1}^{(0)}\kappa^2\left[1+\frac{9}{16}\kappa\left(1-\frac{47}{144}\kappa+\frac{9227}{6912}\kappa^2\right)\right]\frac{x_1x_3}{r^2}$
Deformation-induced lift (equation (37))	$\boldsymbol{F}_M^{(\delta)} \approx \frac{3}{10}\pi\kappa^2\left(1+\frac{3}{2}\kappa\right)(V_{B1}^{(0)})^2\boldsymbol{e}_3$	$\boldsymbol{F}_M^{(\delta)} \approx \frac{171}{320}\pi\kappa^2\left(1+\frac{9}{4}\kappa\right)(V_{B1}^{(0)})^2\boldsymbol{e}_3$
Inertial lift (equation (44))	$\boldsymbol{F}_M^{(G)} \approx \frac{\pi}{4}(V_{B1}^{(0)})^2\{1+0.125\kappa-0.516\kappa^2\}\boldsymbol{e}_3$	$\boldsymbol{F}_M^{(G)} \approx \frac{9\pi}{6}(V_{B1}^{(0)})^2\{1+0.1875\kappa-0.168\kappa^2\}\boldsymbol{e}_3$
(*b*) Drag (equation (23*a*))	$\boldsymbol{F}_{DS} \approx -\frac{\pi}{2}\alpha\kappa^2\left(1+\frac{3}{8}\kappa\right)\boldsymbol{e}_1$	$\boldsymbol{F}_{DS} \approx -\frac{15}{8}\pi\alpha\kappa^2\left(1+\frac{9}{16}\kappa\right)\boldsymbol{e}_1$
Deformation (equation (24))	$f_{2S}^{(\delta)} \approx 2\alpha\left[1+\frac{3}{8}\kappa^3\right]\frac{x_1x_3}{r^2}$	$f_{2S}^{(\delta)} \approx \frac{19}{8}\alpha\left[1+\frac{15}{16}\kappa^3\right]\frac{x_1x_3}{r^2}$
Deformation-induced lift (equation (38))	$\boldsymbol{F}_{MS}^{(\delta)} \approx \left[\frac{4}{5}\pi\alpha V_{S1}^{(0)}\left(1+\frac{3}{8}\kappa+\frac{9}{64}\kappa^2\right)+\frac{169}{70}\alpha^2\kappa^2\right]\boldsymbol{e}_3$	$\boldsymbol{F}_{MS}^{(\delta)} \approx \left[\frac{57}{40}\pi\alpha V_{S1}^{(0)}\left(1+\frac{9}{16}\kappa+\frac{81}{256}\kappa^2\right)+\frac{20463}{4480}\alpha^2\kappa^2\right]\boldsymbol{e}_3$
Inertial lift (equation (47))	$\boldsymbol{F}_{MS}^{(G)} \approx \frac{11}{24}\pi\alpha\left[\frac{\alpha}{3}\left(1+\frac{3}{8}\kappa\right)-V_{S1}^{(0)}\left(\kappa^{-1}+\frac{99}{88}+\frac{45}{44}\kappa\right)\right]\boldsymbol{e}_3$	$\boldsymbol{F}_{MS}^{(G)} \approx \frac{99}{96}\pi\alpha\left[\frac{5\alpha}{9}\left(1+\frac{9}{16}\kappa\right)-V_{S1}^{(0)}\left(\kappa^{-1}+\frac{443}{528}+\frac{52}{55}\kappa\right)\right]\boldsymbol{e}_3$
(*c*) Leading-order Drag (equation (51))	$\boldsymbol{F}_{DC} \approx -4\pi V_{B3}^{(0)}\left[1-\frac{3}{4}\kappa-\frac{9}{64}\kappa^4\right]^{-1}\boldsymbol{e}^3$	$\boldsymbol{F}_{DC} \approx -6\pi V_{B3}^{(0)}\left[1-\frac{9}{8}\kappa+\frac{1}{2}\kappa^3-\frac{135}{256}\kappa^4-\frac{1}{8}\kappa^5\right]^{-1}\boldsymbol{e}_3$ (Fuentes *et al.* 1988)
Deformation (equations (24) and (31))	$f_2^{(\delta)} \approx 2\alpha\left(1+\frac{3}{8}\kappa^3\right)\frac{x_1x_3}{r^2}+\frac{3}{8}V_{B3}^{(0)}\kappa^2\left(1+\frac{3}{4}\kappa\right)\left(3\frac{x_3^2}{r^2}-1\right)$	$f_2^{(\delta)} \approx \frac{19}{9}\alpha\left(1+\frac{15}{16}\kappa^3\right)\frac{x_1x_3}{r^2}+\frac{9}{16}V_{B3}^{(0)}\kappa^2\left(1+\frac{9}{8}\kappa\right)\left(3\frac{x_3^2}{r^2}-1\right)$
Corrections to the drag (equations (52) and (54))	$\left(\delta\boldsymbol{F}_M^{(\delta)}+G\boldsymbol{F}_M^{(G)}\right)\cdot\boldsymbol{e}_3 \approx \frac{3}{10}\pi\delta\kappa^2\left(2(V_{B3}^{(0)})^2+\frac{54}{7}\alpha^2\right)+\frac{11}{72}\pi G\alpha^2$	$\left(\delta\boldsymbol{F}_M^{(\delta)}+G\boldsymbol{F}_M^{(G)}\right)\cdot\boldsymbol{e}_3 \approx \frac{171}{320}\pi\delta\kappa^2\left(3(V_{B3}^{(0)})^2+\frac{54}{7}\alpha^2\right)+\frac{55}{96}\pi G\alpha^2$
Horizontal slip velocity (equation (57))	$V_{S1} \approx -\frac{\alpha}{8}\kappa^2+G\left\{\frac{1}{5}Oh^{-1}-\frac{5}{32}\kappa^{-1}+\frac{83}{384}-\frac{\bar{\rho}}{3}\right\}\alpha V_{B3}^{(0)}$	$V_{S1} \approx -\frac{5}{16}\alpha\kappa^2+G\left\{\frac{19}{80}Oh^{-1}-\frac{15}{64}\kappa^{-1}+\frac{4133}{23040}-\frac{2}{9}\bar{\rho}\right\}\alpha V_{B3}^{(0)}$

TABLE 2. Summary of (*a*) slip-induced effects for the case of a vertical wall, (*b*) shear-induced effects for the case of a vertical wall, (*c*) results for the case of a horizontal wall.

of the present results are accurate down to separation distances between the drop centroid and the wall of about one drop diameter, some of them even providing fairly accurate approximations much closer to the wall. Since the viscosity ratio between the two fluids was kept arbitrary all along the calculations, the expressions derived here show how this ratio influences the various results through the differences in the strength of the stokeslet (R_μ), irrotational dipole (D_μ), and stresslet (R_S) present in the unbounded solution. The main results obtained in the situation of a buoyant drop moving near a vertical wall in a fluid at rest at infinity are summarized in table 2(a) for the two limit cases of an inviscid bubble and a very viscous drop. In this situation the deformation is inversely proportional to the square of the distance to the wall. Inertial and deformation-induced lift forces are both positive, so that both types of particle migrate away from the wall whatever the value of the Ohnesorge number (however our prediction shows that the deformation-induced migration is towards the wall for drops corresponding to an $O(1)$ viscosity ratio). The shear-induced contributions determined in the case of a buoyant drop moving in a linear shear flow near a vertical wall are summarized in table 2(b). The shear rate tends to increase the drag force near the wall, thus resulting in a negative slip velocity for neutrally buoyant particles. The inertial and deformation-induced lift forces involve a positive near-wall contribution proportional to the square of the shear rate, and a term proportional to the product of the shear rate and the slip velocity. The latter contribution may dominate for large enough slip velocities and may then reverse the sign of the migration compared to the case of a neutrally buoyant particle. Finally, results obtained for a buoyant drop moving near a horizontal wall in a fluid at rest or in a linear shear flow are given in table 2(c). Here the wall-induced drag correction is stronger than in the case of a particle moving parallel to the wall, owing to the different near-wall pattern of the streamlines of the disturbance. The net contribution of the inertial and deformation-induced corrections has two components. The vertical one is directed away from the wall, so that it increases (resp. decreases) the drag force on a particle moving towards (resp. away from) the wall. The horizontal contribution modifies the slip velocity in a quite complex way. While the particle always lags behind the fluid for small separations, it may lead it for moderate separations if the deformation is large enough.

These various results are of direct use for computing particle trajectories in the presence of a wall. We think that they may help to improve the modelling of dilute buoyant suspensions in the neighbourhood of solid walls.

J. M. and D. L. are very grateful to Howard A. Stone for helpful discussions on the problems addressed in this work and for his many suggestions that greatly improved the form of the manuscript.

Appendix A

The central point of Faxén's (1921, 1924) technique is the recognition that the fundamental solution of Laplace's equation in free space may be expressed in the integral form

$$\frac{1}{r} = \frac{1}{2\pi} \int_{-\infty}^{+\infty} \int_{-\infty}^{+\infty} \frac{1}{k} \, \mathrm{e}^{\mathrm{i}(\alpha x_1 + \beta x_2) - k|x_3|} \, \mathrm{d}\alpha \, \mathrm{d}\beta, \tag{A 1a}$$

with $k = (\alpha^2 + \beta^2)^{1/2}$ and $\mathrm{i}^2 = -1$ (the wavenumber α must not be confused with the shear rate defined in the main text). Equation (A 1a) may be differentiated at

any order to give higher-order singular solutions. Terms of the form $x_\gamma \nabla^{(n)}(1/r)$ with $n \geqslant 1$ and $x_\gamma = (x_1, x_2)$ are also readily transformed with the help of the identity

$$\int_{-\infty}^{+\infty}\int_{-\infty}^{+\infty} x_\gamma F(\alpha,\beta,k)\,\mathrm{e}^{\mathrm{i}(\alpha x_1+\beta x_2)-k|x_3|}\,\mathrm{d}\alpha\,\mathrm{d}\beta = \mathrm{i}\int_{-\infty}^{+\infty}\int_{-\infty}^{+\infty}\left(\frac{\partial F}{\partial k_\gamma}-\frac{k_\gamma}{k}|x_3|F\right)\mathrm{e}^{\mathrm{i}(\alpha x_1+\beta x_2)-k|x_3|}\,\mathrm{d}\alpha\,\mathrm{d}\beta, \quad (\mathrm{A}\,1b)$$

with $k_\gamma = (\alpha, \beta)$.

Using the above results, Faxén established that any elementary singular velocity field ${}_1\boldsymbol{U}_S$ satisfying Stokes equation may be expressed in the generic form

$$\begin{aligned}{}_1\boldsymbol{U}_S = \frac{1}{2\pi}\int_{-\infty}^{+\infty}\int_{-\infty}^{+\infty}\mathrm{e}^{\mathrm{i}(\alpha x_1+\beta x_2)-k|x_3|}\Bigg\{&\frac{2}{k}g_1\boldsymbol{e}_1+\frac{\mathrm{i}}{k}g_2(\alpha\boldsymbol{e}_1+\beta\boldsymbol{e}_2)\\ &-\frac{x_3}{|x_3|}(g_3\boldsymbol{e}_1+g_2\boldsymbol{e}_3)+\frac{\alpha}{k}x_3\left(g_3(\alpha\boldsymbol{e}_1+\beta\boldsymbol{e}_2)+\mathrm{i}\left(k\frac{x_3}{|x_3|}g_3-g_1\right)\boldsymbol{e}_3\right)\\ &-\frac{\alpha}{k^3}(k|x_3|+1)g_1(\alpha\boldsymbol{e}_1+\beta\boldsymbol{e}_2)\Bigg\}\mathrm{d}\alpha\,\mathrm{d}\beta, \end{aligned} \quad (\mathrm{A}\,2a)$$

where functions g_1 to g_3 are determined by applying transformations (A 1*a*, *b*) to the velocity field under consideration. The corresponding reflection on the wall, ${}_2\boldsymbol{U}_S$, may then be sought in the generic form

$$\begin{aligned}{}_2\boldsymbol{U}_S = \frac{1}{2\pi}\int_{-\infty}^{+\infty}\int_{-\infty}^{+\infty}\mathrm{e}^{\mathrm{i}(\alpha x_1+\beta x_2)-k(x_3+2/\kappa)}\Bigg\{&\frac{2}{k}g_4\boldsymbol{e}_1+\frac{\mathrm{i}}{k}g_5(\alpha\boldsymbol{e}_1+\beta\boldsymbol{e}_2)+\mathrm{i}k\boldsymbol{e}_3)\\ &+\frac{\alpha}{k}x_3(g_6(\alpha\boldsymbol{e}_1+\beta\boldsymbol{e}_2)-\mathrm{i}g_4\boldsymbol{e}_3)-\left(\frac{\alpha}{k^3}g_4(\alpha\boldsymbol{e}_1+\beta\boldsymbol{e}_2)-\frac{\mathrm{i}\alpha}{k}g_6\boldsymbol{e}_3\right)(kx_3+1)\Bigg\}\,\mathrm{d}\alpha\,\mathrm{d}\beta, \end{aligned} \quad (\mathrm{A}\,2b)$$

where the unknown functions g_4 to g_6 are determined by applying the no-slip condition ${}_1\boldsymbol{U}_S + {}_2\boldsymbol{U}_S = \boldsymbol{0}$ at the wall.

Using (A 1*a*, *b*), the unit stokeslet (i.e. that corresponding to $R_\mu = 1$ in (5*a*)), $\boldsymbol{U}_{Sto}$ say, may be recast in the form (A 2*a*) by setting $g_1 = \frac{1}{2}$, $g_2 = g_3 = 0$. Seeking ${}_2\boldsymbol{U}_{Sto}$ in the form (A 2*b*) yields $g_4 = -\frac{1}{2}$, $g_5 = -\mathrm{i}(\alpha/\kappa k)(1-k/\kappa)$, $g_6 = -1/\kappa$. Expanding ${}_2\boldsymbol{U}_{Sto}$ near the drop, i.e. for small values of κr, and keeping terms up to $O(\kappa^3)$ we obtain after performing integrations

$$\begin{aligned}{}_2\boldsymbol{U}_{Sto}(\kappa r \ll 1) = I'_D\boldsymbol{e}_1 + I'_S(x_3\boldsymbol{e}_1+x_1\boldsymbol{e}_3)&\\ +\left(\tfrac{1}{2}(I'_{C2}+I'_{C3})x_1^2+I'_{Q2}x_2^2+I'_{Q3}x_3^2\right)\boldsymbol{e}_1&\\ -I'_{C2}x_1x_2\boldsymbol{e}_2-I'_{C3}x_1x_3\boldsymbol{e}_3+O(\kappa^4),& \end{aligned} \quad (\mathrm{A}\,3a)$$

with

$$I'_D = -\tfrac{3}{8}\kappa, \quad I'_S = \tfrac{3}{16}\kappa^2, \quad I'_{Q2} = \tfrac{5}{64}\kappa^3, \quad I'_{Q3} = -\tfrac{1}{16}\kappa^3,$$
$$I'_{C2} = -\tfrac{1}{32}\kappa^3, \quad I'_{C3} = \tfrac{1}{4}\kappa^3. \quad (\mathrm{A}\,3b)$$

Similarly, expressing the unit irrotational dipole $\boldsymbol{U}_D$ of (5*a*) within Faxén's form we find $g_1 = g_3 = 0$, $g_2 = -\mathrm{i}\alpha|x_3|$, and the image ${}_2\boldsymbol{U}_D$ with respect to the wall is obtained by setting $g_4 = 0$, $g_5 = \mathrm{i}\alpha(1-2k/\kappa)$, $g_6 = 2k$ in (A 2*b*). Expanding ${}_2\boldsymbol{U}_D$ in the vicinity of the drop and keeping terms of $O(\kappa^4)$ and $O(\kappa^5)$ in view of the higher-order

approximation derived in § 3.3, we obtain

$$
\begin{aligned}
{}_2\boldsymbol{U}_D(\kappa r \ll 1) = {} & I_0\boldsymbol{e}_1 + I_{DS}(x_3\boldsymbol{e}_1 + x_1\boldsymbol{e}_3) + I_{DR}(x_3\boldsymbol{e}_1 - x_1\boldsymbol{e}_3) \\
& + \left[\tfrac{1}{2}(I_{DC2} + I_{DC3})x_1^2 + I_{DQ2}x_2^2\right]\boldsymbol{e}_1 \\
& - I_{DC2}x_1x_2\boldsymbol{e}_2 - I_{DC3}x_1x_3\boldsymbol{e}_3 + O(\kappa^6),
\end{aligned} \tag{A 4a}
$$

with

$$
\begin{gathered}
I_0 = \tfrac{1}{4}\kappa^3, \quad I_{DS} = -\tfrac{9}{16}\kappa^4, \quad I_{DR} = \tfrac{3}{8}\kappa^4, \quad I_{DQ2} = -\tfrac{3}{16}\kappa^5, \\
I_{DC2} = \tfrac{3}{8}\kappa^5, \quad I_{DC3} = -\tfrac{3}{2}\kappa^5.
\end{gathered} \tag{A 4b}
$$

The velocity field corresponding to the unit stresslet in (8a), $\boldsymbol{U}_{Str}$ say, is recast within the form (A 2a) by setting $g_1 = g_2 = 0$, $g_3 = -\frac{1}{3}$ and we find that the image ${}_4\boldsymbol{U}_{Str}$ of $\boldsymbol{U}_{Str}$ corresponds to $g_4 = k/6$, $g_5 = -(2\mathrm{i}\alpha/3\kappa)(-1 + \kappa/4k + k/\kappa)$, $g_6 = -\frac{1}{6}(1 - 4k/\kappa)$ in (A 2b). The velocity field ${}_4\boldsymbol{U}_{str}$ may then be expanded in the vicinity of the drop as

$$
{}_4\boldsymbol{U}_{Str}(\kappa r \ll 1) = I_{SD}\boldsymbol{e}_1 + I_{SS}(x_3\boldsymbol{e}_1 + x_1\boldsymbol{e}_3) + I_{SR}(x_3\boldsymbol{e}_1 - x_1\boldsymbol{e}_3) + O(\kappa^4), \tag{A 5a}
$$

with

$$
I_{SD} = \tfrac{1}{8}\kappa^2, \quad I_{SS} = -\tfrac{3}{16}\kappa^3, \quad I_{SR} = \tfrac{1}{16}\kappa^3. \tag{A 5b}
$$

In the complementary problem (§ 4), the unit stokeslet (corresponding to $R_\mu = 1$) in (26a), $\boldsymbol{u}_{Sto}$ say, may be recast within the form (A 2a) by setting $g_1 = \mathrm{i}/2\alpha x_3$, $g_2 = x_3/2$, $g_3 = \mathrm{i}/\alpha k x_3$, so that we obtain $g_4 = 0$, $g_5 = k/\kappa^2$, $g_6 = \frac{\mathrm{i}}{2\alpha}(1 + 2k/\kappa)$ in (A 2b). Similarly, the unit dipole $\boldsymbol{u}_D$ in (26a) corresponds to $g_1 = g_3 = 0$, $g_2 = kx_3/|x_3|$, and its reflection on the wall is found by setting $g_4 = 0$, $g_5 = k(1 - 2k/\kappa)$, $g_6 = -2\mathrm{i}k^2/\alpha$ in (A 2b). Then the images of the stokeslet and dipole are respectively found to be

$$
\begin{aligned}
{}_2\boldsymbol{u}_{Sto}(\kappa r \ll 1) = {} & J'_D\boldsymbol{e}_3 + J'_S(\boldsymbol{x} - 3x_3\boldsymbol{e}_3) \\
& - J'_C(x_1x_3\boldsymbol{e}_1 + x_2x_3\boldsymbol{e}_2) + (J'_Cx_3^2 + J'_Q(x_1^2 + x_2^2))\boldsymbol{e}_3 + O(\kappa^4),
\end{aligned} \tag{A 6a}
$$

with

$$
J'_D = -\tfrac{3}{4}\kappa, \quad J'_S = -\tfrac{3}{16}\kappa^2, \quad J'_Q = \tfrac{5}{16}\kappa^3, \quad J'_C = -\tfrac{1}{8}\kappa^3 \tag{A 6b}
$$

and

$$
\begin{aligned}
{}_2\boldsymbol{u}_D(\kappa r \ll 1) = {} & J_0\boldsymbol{e}_3 + J_{DS}(\boldsymbol{x} - 3x_3\boldsymbol{e}_3) - J_{DC}x_3(x_1\boldsymbol{e}_1 + x_2\boldsymbol{e}_2) \\
& + [J_{DC}x_3^2 + J_{DQ}(x_1^2 + x_2^2)]\boldsymbol{e}_3 + O(\kappa^6),
\end{aligned} \tag{A 7a}
$$

with

$$
J_0 = \kappa^3, \quad J_{DS} = \tfrac{9}{16}\kappa^4, \quad J_{DC} = \tfrac{3}{4}\kappa^5, \quad J_{DQ} = -\tfrac{9}{8}\kappa^5. \tag{A 7b}
$$

To obtain the $O(\kappa^4)$ correction to the drag force in the case of a drop moving perpendicular to the wall, we also need the image ${}_4\boldsymbol{u}_{Str}$ of the stresslet in (28a). This image corresponds to $g_4 = 0$, $g_5 = k(1 - 2k/\kappa + 2k^2/\kappa^2)$, $g_6 = -\mathrm{i}(k/\alpha)(1 - 2k/\kappa)$ in (A 2b). Thus, performing integrations we obtain

$$
{}_4\boldsymbol{u}_{Str}(\kappa r \ll 1) = J_{SD}\boldsymbol{e}_3 + J_{SS}(\boldsymbol{x} - 3x_3\boldsymbol{e}_3) + O(\kappa^4), \tag{A 8a}
$$

with

$$
J_{SD} = -\tfrac{3}{4}\kappa^2, \quad J_{SS} = -\tfrac{1}{2}\kappa^3. \tag{A 8b}
$$

Appendix B

The prefactors involved in (15*a–c*) are

$$K_{SD} = \sum_{n=0}^{n=5}(-1)^n I_D^n - D_\mu(I_0 + K_D)(1 - 2I_D + 3I_D^2) + 2I_S R_S I_{SD}(1 - 2I_D)$$

$$-\frac{D_\mu^2}{R_\mu}K_{DD} + O(\kappa^6), \tag{B 1}$$

$$K_{SS} = I_S\left[\sum_{n=0}^{3}(-1)^n I_D^n - 2R_S I_{SS}\right] + D_\mu[I_{DS}(1 - I_D) - (I_0 + K_D)I_S] + O(\kappa^6), \tag{B 2}$$

$$K_R = D_\mu I_{DR}(1 - I_D) - 2R_S I_S I_{SR} + O(\kappa^6), \tag{B 3}$$

$$K_{SO} = \sum_{n=0}^{2}(-1)^n I_D^n + O(\kappa^3), \tag{B 4}$$

with $K_{DD} = I_{DC2} + I_{DC3} + 2I_{DQ2} = -\frac{3}{2}\kappa^5$, K_D being defined in § 3.1 just below (8*b*). In (B 1), the various prefactors involving I_D may be considered as the first terms of an infinite series, so that K_{SD} may be written approximatively in the fractional form

$$K_{SD} \approx \frac{1}{1 + I_D + D_\mu(I_0 + K_D) - 2I_S R_S I_{SD} + (D_\mu^2/R_\mu)K_{DD}}. \tag{B 5}$$

These results may be easily transposed to the case of a drop moving perpendicularly to the wall. Using the coefficients given by (A 6*b*), (A 7*b*) and (A 8*b*) we find that the counterpart of (B 5) is

$$K_{SDC} \approx \frac{1}{1 + J_D + D_\mu(J_0 + K_{DC}) - J_S R_S J_{SD} + (D_\mu^2/R_\mu)K_{DDC}}, \tag{B 6}$$

with $K_{DDC} = 2(J_{DC} + +2J_{DQ}) = -3\kappa^5$, K_{DC} being defined in the main text just below (28*b*). Similarly the counterpart of (B 2) giving the strength of the model-2 deformation is

$$K_{SSC} = J_S\left[\sum_{n=0}^{3}(-1)^n J_D^n - 2R_S J_{SS}\right] + D_\mu[J_{DS}(1 - J_D) - (J_0 + K_{DC})J_S] + O(\kappa^6). \tag{B 7}$$

Appendix C

To obtain the expression for $\bar{\boldsymbol{U}}^{(0)}$ and $\bar{\boldsymbol{u}}$ valid in the whole fluid domain, the key step is the determination of the image fields ${}_2\bar{\boldsymbol{U}}^{(0)}$ and ${}_2\bar{\boldsymbol{u}}$. We illustrate the corresponding technique on the case of the image ${}_2\boldsymbol{U}_{Sto}$ of the unit stokeslet involved in the fundamental solution (5*a*). Replacing the functions g_4 to g_6 in (A 2*b*) by their expressions, defining the outer variables $\bar{x}_i = \kappa x_i$ $(i = 1, 3)$, $\bar{r} = \kappa r$, the associated wavenumbers $\bar{k} = k/\kappa$, $\bar{\alpha} = \alpha/\kappa$, $\bar{\beta} = \beta/\kappa$, and changing to polar coordinates allows

us to write ${}_2\boldsymbol{U}_{Sto}$ in the form

$$
\begin{aligned}
{}_2\bar{\boldsymbol{U}}_{Sto} = \frac{\kappa}{2}\int_0^{\infty} \mathrm{e}^{-\bar{k}(\bar{x}_3+2)} \Bigg\{ & \tfrac{1}{2}J_0(\bar{k}\bar{\rho})\left(-\tfrac{3}{2}+\frac{\bar{k}}{2}(2+\bar{x}_3)-\bar{k}^2(1+\bar{x}_3)\right)\boldsymbol{e}_1 \\
& + J_2(\bar{k}\bar{\rho})\left(\tfrac{1}{2}+\bar{k}\left(1+\frac{\bar{x}_3}{2}\right)-\bar{k}^2(1+\bar{x}_3)\right)\left(\tfrac{1}{2}\frac{\bar{x}_2^2-\bar{x}_1^2}{\bar{\rho}^2}\boldsymbol{e}_1-\frac{\bar{x}_1\bar{x}_2}{\bar{\rho}^2}\boldsymbol{e}_2\right) \\
& + \frac{\bar{x}_1}{\bar{\rho}}J_1(\bar{k}\bar{\rho})\left(-\bar{k}\frac{\bar{x}_3}{2}+\bar{k}^2(1+\bar{x}_3)\right)\boldsymbol{e}_3\Bigg\}\,\mathrm{d}\bar{k}
\end{aligned}
\tag{C 1}
$$

with $\bar{\rho}=(\bar{x}_1^2+\bar{x}_2^2)^{1/2}$, $J_n(\bar{k}\bar{\rho})$ being the Bessel function of the first kind of order n. The latter expression can be integrated analytically (Gradshteyn & Ryzhik 1980, p. 712), yielding

$$
{}_2\bar{\boldsymbol{U}}_{Sto} = \frac{\kappa}{2}\left\{-\left(\frac{\boldsymbol{e}_1}{\bar{\tau}}+\frac{\bar{x}_1\bar{\boldsymbol{x}}}{\bar{\tau}^3}\right)+2\frac{1+\bar{x}_3}{\bar{\tau}^5}[(3\bar{x}_1(\bar{\boldsymbol{x}}+2\boldsymbol{e}_3)-\bar{\tau}^2\boldsymbol{e}_1)]\right\},
\tag{C 2}
$$

with $\bar{\tau}=(\bar{\rho}^2+(\bar{x}_3+2)^2)^{1/2}$ and $\bar{\boldsymbol{x}}=\bar{x}_1\boldsymbol{e}_1+\bar{x}_2\boldsymbol{e}_2+\bar{x}_3\boldsymbol{e}_3$. Applying similar techniques to other contributions in (5*a*), (7)–(8*a*), we finally obtain the required approximation of $\bar{\boldsymbol{U}}^{(0)}$ for the case where the fluid is at rest at infinity in the form

$$
\begin{aligned}
\bar{\boldsymbol{U}}^{(0)} = V_{B1}^{(0)}\Bigg[& -\boldsymbol{e}_1+\frac{\kappa}{2}R_\mu\left(\sum_{n=0}^{2}(-1)^n I_D^n\right)\left\{\left(\frac{\boldsymbol{e}_1}{\bar{r}}+\frac{\bar{x}_1\bar{\boldsymbol{x}}}{\bar{r}^3}\right)-\left(\frac{\boldsymbol{e}_1}{\bar{\tau}}+\frac{\bar{x}_1\bar{\boldsymbol{x}}}{\bar{\tau}^3}\right)\right. \\
& \left.+2\frac{1+\bar{x}_3}{\bar{\tau}^5}(3\bar{x}_1(\bar{\boldsymbol{x}}+2\boldsymbol{e}_3)-\bar{\tau}^2\boldsymbol{e}_1)\right\}+\kappa^3 D_\mu\left\{\left(\frac{\boldsymbol{e}_1}{\bar{r}^3}-3\frac{\bar{x}_1\bar{\boldsymbol{x}}}{\bar{r}^5}\right)-\left(\frac{\boldsymbol{e}_1}{\bar{\tau}^3}-3\frac{\bar{x}_1\bar{\boldsymbol{x}}}{\bar{\tau}^5}\right)\right. \\
& \left.+\left(6\frac{(1+\bar{x}_3)(2+\bar{x}_3)}{\bar{\tau}^7}[(\bar{\tau}^2\boldsymbol{e}_1-5\bar{x}_1(\bar{\boldsymbol{x}}+2\boldsymbol{e}_3))]\right\}\Bigg]+O(\kappa^4)\,.
\end{aligned}
\tag{C 3}
$$

By similar techniques we find that the expression of the complementary velocity $\bar{\boldsymbol{u}}$ is

$$
\begin{aligned}
\bar{\boldsymbol{u}} = -\boldsymbol{e}_3+\frac{\kappa}{2}R_\mu\left(\sum_{n=0}^{2}(-1)^n J_D^n\right)\Bigg\{ & \left(\frac{\boldsymbol{e}_3}{\bar{r}}+\frac{\bar{x}_3\bar{\boldsymbol{x}}}{\bar{r}^3}\right)\left(\frac{\boldsymbol{e}_3}{\bar{\tau}}+\frac{\bar{x}_3\bar{\boldsymbol{x}}}{\bar{\tau}^3}\right)-2\frac{1+\bar{x}_3}{\bar{\tau}^5} \\
& \times(3(\bar{x}_3+2)(\bar{\boldsymbol{x}}+2\boldsymbol{e}_3)+\bar{\tau}^2\boldsymbol{e}_3)\Bigg\}+\kappa^3 D_\mu\left\{\left(\frac{\boldsymbol{e}_3}{\bar{r}^3}-3\frac{\bar{x}_3\bar{\boldsymbol{x}}}{\bar{r}^5}\right)-\left(\frac{\boldsymbol{e}_3}{\bar{\tau}^3}+3\frac{(\bar{x}_3+2)\bar{\boldsymbol{x}}}{\bar{\tau}^5}\right)\right. \\
& \left.-6\frac{1+\bar{x}_3}{\bar{\tau}^7}((\bar{\tau}^2-5(\bar{x}_3+2)^2)(\bar{\boldsymbol{x}}+2\boldsymbol{e}_3)+(\bar{x}_3+2)\bar{\tau}^2\boldsymbol{e}_3)\right\}+O(\kappa^4).
\end{aligned}
\tag{C 4}
$$

In the case of a linear shear flow, the $O(\kappa^3)$-approximation of $\bar{\boldsymbol{U}}^{(0)}$ involves the image of the stresslet. Having determined this elementary solution, the prefactors are

readily identified in § 3.4. Hence we obtain

$$\bar{\boldsymbol{U}}^{(0)} = (\kappa^{-1}\alpha\bar{x}_3 - V_{S1}^{(0)})\boldsymbol{e}_1 + \frac{\kappa}{2}R_\mu\left(V_{S1}^{(0)}\sum_{n=0}^{2}(-1)^n I_D^n + \alpha R_S I_{SD}\right)$$
$$\times\left\{\left(\frac{\boldsymbol{e}_1}{\bar{r}} + \frac{\bar{x}_1\bar{\boldsymbol{x}}}{\bar{r}^3}\right) - \left(\frac{\boldsymbol{e}_1}{\bar{\tau}} + \frac{\bar{x}_1\bar{\boldsymbol{x}}}{\bar{\tau}^3}\right) + 2\frac{1+\bar{x}_3}{\bar{\tau}^5}(3\bar{x}_1(\bar{\boldsymbol{x}}+2\boldsymbol{e}_3) - \bar{\tau}^2\boldsymbol{e}_1)\right\}$$
$$+\kappa^3 D_\mu V_{S1}^{(0)}\left\{\left(\frac{\boldsymbol{e}_1}{\bar{r}^3} - 3\frac{\bar{x}_1\bar{\boldsymbol{x}}}{\bar{r}^5}\right) - \left(\frac{\boldsymbol{e}_1}{\tau^3} - 3\frac{\bar{x}_1\bar{\boldsymbol{x}}}{\bar{\tau}^5}\right) + 6\frac{(1+\bar{x}_3)(2+\bar{x}_3)}{\bar{\tau}^7}\right.$$
$$\left.\times[(\bar{\tau}^2\boldsymbol{e}_1 - 5\bar{x}_1(\bar{\boldsymbol{x}}+2\boldsymbol{e}_3))]\right\} - 2\kappa^2 R_S\alpha\left\{\left(\frac{\bar{x}_3}{\bar{r}^5} + \frac{2+\bar{x}_3}{\bar{\tau}^5}\right)\bar{x}_1\bar{\boldsymbol{x}}\right.$$
$$\left.+2\frac{1+\bar{x}_3}{\bar{\tau}^7}[\bar{\tau}^2((2+\bar{x}_3)\boldsymbol{e}_1 + \bar{x}_1\boldsymbol{e}_3) - 5\bar{x}_1(2+\bar{x}_3)(\bar{\boldsymbol{x}}+2\boldsymbol{e}_3)]\right\} + O(\kappa^4). \quad \text{(C 5)}$$

REFERENCES

Ambari, A., Gauthier-Manuel, B. & Guyon, E. 1983 Effect of a plane wall on a sphere moving parallel to it. *J. Phys. Lett.* **44**, 143–146.

Ascoli, E. P., Dandy, D. S. & Leal, L. G. 1990 Buoyancy-driven motion of a deformable drop toward a planar wall at low Reynolds number. *J. Fluid Mech.* **213**, 287–311.

Batchelor, G. K. 1967 *An Introduction to Fluid Dynamics*. Cambridge University Press.

Becker, L. E., McKinley, G. H. & Stone, H. A. 1996 Sedimentation of a sphere near a plane wall: weak non-Newtonian and inertial effects. *J. Non-Newtonian Fluid Mech.* **63**, 201–233.

Brenner, H. 1961 The slow motion of a sphere through a viscous flow towards a plane surface. *Chem. Engng Sci.* **16**, 242–251.

Bretherton, F. P. 1962 The motion of rigid particles in a shear flow at low Reynolds number. *J. Fluid Mech.* **14**, 284–304.

Chaffey, C. E., Brenner, H. & Mason, S. G. 1965 Particle motions in sheared suspensions XVIII: Wall migration (theoretical). *Rheol. Acta* **4**, 64–72; and Corrections. *Rheol. Acta* **6**, 100, 1967.

Chan, P. C. H. & Leal, L. G. 1977 A note on the motion of a spherical particle in a general quadratic flow of a second-order fluid. *J. Fluid Mech.* **82**, 549–559.

Chan, P. C. H. & Leal, L. G. 1979 The motion of a deformable drop in a second-order fluid. *J. Fluid Mech.* **92**, 131–170.

Chan, P. C. H. & Leal, L. G. 1981 An experimental study of drop migration in shear flow between concentric cylinders. *Intl J. Multiphase Flow* **7**, 83–99.

Cherukat, P. & McLaughlin, J. B. 1990 Wall-induced lift on a sphere. *Intl J. Multiphase Flow* **16**, 899–907.

Cherukat, P. & McLaughlin, J. B. 1994 The inertial lift on a rigid sphere in a linear shear flow field near a flat wall. *J. Fluid Mech.* **263**, 1–18.

Chervenivanova, E. & Zapryanov, Z. 1985 On the deformation of two droplets in a quasisteady Stokes flow. *Intl J. Multiphase Flow* **11**, 721–738.

Clift, R., Grace, J. R. & Weber, M. E. 1978 *Bubbles, Drops and Particles*. Academic.

Cox, R. G. 1969 The deformation of a drop in a general time-dependent fluid flow. *J. Fluid Mech.* **37**, 601–623.

Cox, R. G. & Brenner, H. 1968 The lateral migration of solid particles in Poiseuille flow: 1. Theory. *Chem. Engng Sci.* **23**, 147–173.

Cox, R. G. & Hsu, S. K. 1977 The lateral migration of solid particles in a laminar flow near a plate. *Intl J. Multiphase Flow* **3**, 201–222.

Faxén, H. 1921 Einwirkung der gerfäßwände auf den Widerstand gegen die bewegung einer kleinen kugel in einer zähen flüssigkeit. PhD Dissertation, University of Upsala.

Faxén, H. 1924 Der widerstand gegen die bewegung einer starren kugel in einer zähen flüssigkeit

die zwischen zwei parallelen ebenen wänden eingeschlossen ist. *Ark. Matematik, Astronomi och Fysik* **18**, 1–52.

Fisher, T. M. & Rosenberger, R. 1987 A boundary integral method for the numerical computation of the forces exerted on a sphere in viscous incompressible flows near a plane wall. *Z. Angew. Math. Phys.* **38**, 339–365.

Frankel, N. A. & Acrivos, A. 1970 The constitutive equation for a dilute emulsion. *J. Fluid Mech.* **44**, 65–78.

Fuentes, Y. O., Kim, S. & Jeffrey, D. J. 1988 Mobility functions for two unequal viscous drops in Stokes flow. I. Axisymmetric motions. *Phys. Fluids* **31**, 2445–2455.

Goldman, A. J., Cox, R. G. & Brenner, H. 1967 Slow viscous motion of a sphere parallel to a plane wall. Part I. Motion through a quiescent liquid. *Chem. Engng Sci.* **22**, 637–651.

Gradshteyn, I. S. & Ryzhik, I. M. 1980 *Table of Integrals, Series and Products*. Academic.

Halow, J. S. & Wills, G. B. 1970 Radial migration of spherical particles in Couette systems. *AIChE J.* **16**, 281–286.

Happel, J. & Brenner, H. 1973 *Low Reynolds Number Hydrodynamics*. Martinus Nijhoff.

Harper, E. Y. & Chang, I. D. 1968 Maximum dissipation resulting from lift in a slow viscous shear flow. *J. Fluid Mech.* **33**, 209–225.

Hetsroni, G. & Haber, S. 1970 Flow in and around a droplet or bubble submerged in an unbounded arbitrary velocity field. *Rheol. Acta* **9**, 488–496.

Ho, B. P. & Leal, L. G. 1974 Inertial migration of rigid spheres in two-dimensional unidirectional flows. *J. Fluid Mech.* **65**, 365–400.

Hogg, A. J. 1994 The inertial migration of non-neutrally buoyant spherical particles in two-dimensional shear flows. *J. Fluid Mech.* **272**, 285–318.

Karnis, A., Goldsmith, H. L. & Mason, S. G. 1966 The kinetics of flowing dispersions. I. Concentrated suspensions of rigid particles. *J. Colloid Interface Sci.* **22**, 531–553.

Karnis, A. & Mason, S. G. 1967 Particle motion in sheared suspensions. Wall migration of fluid drops. *J. Colloid Interface Sci.* **24**, 164–169.

Kim, S. & Karrila, S. J. 1991 *Microhydrodynamics. Principles and Selected Applications*. Butterworth–Heinemann.

Krishnan, G. P. & Leighton, D. T. 1995 Inertial lift on a moving sphere in contact with a plane wall in a shear flow. *Phys. Fluids* **7**, 2538–2545.

Leal, L. G. 1980 Particle motions in a viscous fluid. *Annu. Rev. Fluid Mech.* **12**, 435–476.

Leal, L. G. 1992 *Laminar Flow and Convective Transport Processes*. Butterworth–Heinemann.

Legendre, D. & Magnaudet, J. 1997 A note on the lift force on a bubble or a drop in a low-Reynolds-number shear flow. *Phys. Fluids* **9**, 3572–3574.

Leighton, D. T. & Acrivos, A. 1985 The lift force on a small sphere touching a plane in the presence of a simple shear flow. *Z. Angew. Math. Phys.* **36**, 174–178.

Lorentz, H. A. 1896 Ein allgemeiner satz, die bewengung einer reibendon flüssigkeit bettrefend, nebst einigen anwendungen desselben. *Versl. Kon. Akad. Wetensch. Amsterdam* **5**, 168–174.

Lovalenti, P. M. & Brady, J. F. 1993 The hydrodynamic force on a rigid particle undergoing arbitrary time-dependent motion at small Reynolds number. *J. Fluid Mech.* **256**, 561–605.

Manga, M. & Stone, H. A. 1993 Buoyancy-driven interactions between two deformable viscous drops. *J. Fluid Mech.* **256**, 647–683.

McLaughlin, J. B. 1993 The lift on a small sphere in wall-bounded linear shear flows. *J. Fluid Mech.* **246**, 249–265.

O'Neill, M. E. & Stewarson, K. 1967 On the slow motion of a sphere parallel to a nearby plane wall. *J. Fluid Mech.* **27**, 706–724.

Saffman, P. G. 1965 The lift force on a small sphere in a slow shear flow. *J. Fluid Mech.* **22**, 385–400.

Schonberg, J. A. & Hinch, E. J. 1989 Inertial migration of a sphere in Poiseuille flow. *J. Fluid Mech.* **203**, 517–524.

Segré, G. & Silberberg, A. 1962*a* Behaviour of macroscopic rigid spheres in Poiseuille flow. Part 1. Determination of local concentration by statistical analysis of particle passages through crossed light beams. *J. Fluid Mech.* **14**, 115–135.

Segré, G. & Silberberg, A. 1962*b* Behaviour of macroscopic rigid spheres in Poiseuille flow. Part 2. Experimental results and interpretation. *J. Fluid Mech.* **14**, 136–157.

Shapira, M. & Haber, S. 1988 Low Reynolds number motion of a droplet between two parallel plates. *Intl J. Multiphase Flow* **14**, 483–506.

Smart, J. R. & Leighton, D. T. 1991 Measurement of the drift of a droplet due to the presence of a plane. *Phys. Fluids* A **3**, 21–28.

Stone, H. A. 2000 Philip Saffman and viscous flow theory. *J. Fluid Mech.* **409**, 165–183.

Takemura, F., Takagi, S., Magnaudet, J. & Matsumoto, Y. 2002 Drag and lift forces on a bubble rising near a vertical wall in a viscous liquid. *J. Fluid Mech.* **461**, 277–300.

Taylor, G. I. 1932 The viscosity of fluid containing small drops of another fluid. *Proc. R. Soc. Lond.* A **138**, 41–48.

Taylor, G. I. 1934 The formation of emulsions in definable fields of flow. *Proc. R. Soc. Lond.* A **146**, 501–523.

Taylor, T. D. & Acrivos, A. 1964 On the deformation and drag of a falling viscous drop at low Reynolds number. *J. Fluid Mech.* **18**, 466–476.

Uijttewaal, W. S. J. & Nijhof, E. 1995 The motion of a droplet subjected to linear shear flow including the presence of a plane wall. *J. Fluid Mech.* **302**, 45–63.

Uijttewaal, W. S. J., Nijhof, E. & Heethaar, R. M. 1993 Droplet migration, deformation, and orientation in the presence of a plane wall: a numerical study compared with analytical theories. *Phys. Fluids* A **5**, 819–825.

Vasseur, P. & Cox, R. G. 1976 The lateral migration of a spherical particle in two-dimensional shear flows. *J. Fluid Mech.* **78**, 385–413.

Vasseur, P. & Cox, R. G. 1977 The lateral migration of spherical particles sedimenting in a stagnant bounded fluid. *J. Fluid Mech.* **80**, 561–591.